UNIVERSITY
OF OULU

Faculty of Technology

Master of Science (Technology) in Environmental Engineering

Accuracy assessment of Remote Sensing altimetry: An Integrated approach of Lake Water Level response.

Author: Mehedi Rabbil

Supervisors:

Dr. Ali Torabi Haghighi

MSc. Joy Bhattacharjee

Master's Thesis

September 2019

ABSTRACT

For Thesis   University of Oulu Faculty of Technology

Degree Programme (Bachelor's Thesis, Master's Thesis) Barents Environmental Engineering	Major Subject (Licentiate Thesis) Water, Energy and Environmental Engineering
Author Rabbil, Mehedi	Thesis Supervisors Torabi Haghighi, Ali; Bhattacharjee, Joy

Title of Thesis
Accuracy assessment of Remote Sensing altimetry: An Integrated approach of Lake Water Level response.

Major Subject Water and Environment	Type of Thesis Master's Thesis	Submission Date September 2019	Number of Pages 46 Pages

Abstract

Declination of lake water levels are extensively influenced by anthropogenic activities along with basin size, topography, and lake size. Lake Urmia was one of the largest hypersaline lakes in north-west Iran. Main outflow from the lake are evaporation and possible groundwater flux, whereas major sources of inflow are surrounding rivers and several streams. Overall, annual evaporation is higher than precipitation. The lake Water Level Fluctuation (WLF) is a function of inflow, rainfall, evaporation and groundwater flux. The aim of this study is to assess the accuracy of different Remote Sensing (RS) data which influences on WLF. Variation of Lake Urmia WLF in several sections were estimated based on different satellite missions e.g. Jason-2 and Jason-3 and compared with observed data and DAHITI dataset. The outcome showed that the algorithm of estimated WLF indicates better outline in some sections in Lake Urmia while some cases are not in good harmony with observed and DAHITI data. In order to find RS data accuracy, different driving factors on WLF were integrated by applying Water Balance simulation with combination of different scenarios for 2003-2007. The results showed the scenario which combines all observed data, has best pattern with observed Water Level of the lake to explain the response of the lake.

Additional Information

TABLE OF CONTENTS

FOREWORD

First and foremost, I would like to express my sincerer gratitude and most enormous thanks to my advisor Dr. Ali Torabi Haghighi for his theoretical guidance, cordial support, patience and encouragement during my studies at the University of Oulu. I would also like to express my most profound appreciation and gratitude to my second advisor, MSc. Joy Bhattacharjee for his valuable guidance, inspiration and exceptional support throughout this journey. This master's thesis would have been really impossible without his help and I am undoubtedly indebted to him.

I am grateful at the Water, Energy and Environmental Engineering Research Group at the University of Oulu for the opportunity of meeting excellent academics. Many thanks to my honourable teacher Dr. Anna-Kaisa Ronkanen, who taught me precious knowledge during two years of studying at the University of Oulu. I also appreciate my friend Abol Fazl, Mouad and Janne for their contribution during two years of my studies at the University of Oulu.

I would like to show my deepest gratitude to my family and especially to my beloved parents and spouse for their unbelievable encouragement and continuous prayers throughout the journey.

Oulu, September 26, 2019

Mehedi Rabbil

LIST OF ABBREVIATIONS AND SYMBOLS

RS	Remote Sensing
WLF	Water Level Fluctuations
DAHITI	Database for Hydrological Time Series of Inland Waters
J-2	JASON-2
J-3	JASON-3
MODIS	Moderate Resolution Imaging Spectroradiometer
USGS	United States Geological Survey
NASA	The National Aeronautics and Space Administration
NOAA	The National Oceanic and Atmospheric Administration
CNES	The National Centre for Space Studies
GDR	Geophysical Data Records
IGDR	Interim Geophysical Data Records
NDWI	The Normalized Difference Water Index
SSEBop	Operational Simplified Surface Energy Balance
SEBAL	Surface Energy Balance Algorithm for Land
SEBS	Surface Energy Balance System
TOA	Top of Atmosphere
LE	Latent Heat Fluxes
NIR	Near-infrared
ERS1	European Remote Sensing Satellite
Geosat	Geophysical Satellite

1 INTRODUCTION

There are millions of lakes as well as reservoirs that exist on this earth. To meet water resources demand, numerous dams were also constructed in last 100 years (Richter & Thomas, 2007; Rosenberg, 2000; WCD, 2000). Inland water bodies, particularly lakes and rivers are the main contributions of freshwater resources. Inadequate water resources management, anthropogenic activities and climate change effect the natural flow pattern of lakes and rivers (Torabi Haghighi & Kløve, 2015a). Several factors have effected lake hydrology, ecology and ecosystem (Torabi Haghighi & Kløve, 2015a) for many years. Lake Water Level Fluctuations (WLF) also occurred due to natural conditions in different temporal scales (Chow-Fraser, 2005; Hofmann et al., 2008). Although, several lake system have high water level variations because of intensive evaporation and inflow variations rather than other lakes (Torabi Haghighi & Kløve, 2017b).

The number of observed hydrological gauging stations are globally decreasing around the world. For instance, in 1978 total observed stations were approximately 8,000, but in 2013 that became 1000 (GRDC, 2013, Tuiran et al., 2013a). In developing countries, the data accessibility is even more difficult due to instable economic and political situation. In comparison to observed dataset, remote sensing dataset are widely used these days because of accessibility, and spatial coverage. Multi-mission remote sensing altimetry can be used to estimate water level variations and water storage volume. For example, with application of specific algorithm for satellite altimeter missions, daily water level changes can be estimated (Schwatke et al., 2015a).

Changes in water level can be caused by the changes in water balance components like evaporation, rainfall, and inflow and groundwater flux. Evaporation is one of the substantial and effective components of water budget of a lake, even small amount of actual evaporation change can impact lot in water balance cycle (Abreham, 2009; Laurens et al., 2008). Lake evaporation rate is dependent on solar radiation, wind speed, temperature, atmospheric pressure and lake surrounding environment (Melesse et al., 2009). Estimating evaporation of large water bodies require multiple number of satellite images to have spatial coverage. Such dataset is not available at desired scales in remote areas whereas observed dataset may also contain some errors because of environmental impacts (e.g. atmospheric pressure, wind speed, etc.). To overcome these limitations, it

is essential to use a simple approach that will estimate evaporation based on advanced remote sensing techniques for large water bodies.

Operational Simplified Surface Energy Balance (SSEBop), Surface Energy Balance Algorithm for Land (SEBAL) and Surface Energy Balance System (SEBS) models with integration of USGS MODIS dataset lead to an innovative perception to fill the gap of evaporation estimation. Simplified Surface Energy Balance for operational applications (SSEBop) is based on SSEB approach (Senay et al., 2007a) and has been parameterized for operational applications. Compared to other methods, it is simpler because of less data requirements and provides substantial accuracy to estimate evaporation (Mcshane et al., 2017). It applies predefined boundary conditions that are unique to each pixel according to 'hot' and 'cold' reference environment. In addition, the SSEBop model based results are measurable from pixel to basin scale (Velpuri et al., 2013). In this study, one of the objectives is to consider SSEBop model with USGS MODIS dataset to estimate evaporation.

Monitoring lake water surface areas and its changes is essential in order to understand the lake water level variations (Ecenur, 2016). Fluctuation of lake areas mainly depend on effect of rainfall and evaporation (Torabi Haghighi, et al.,2016b). Remote sensing imagery has been used extensively in many studies to analyse lake water level response (Rokni et al., 2014). Advanced application of remote sensing provides higher possibilities to detect and extract database to monitor open water surface (Xu, 2006). Moreover, accessibility of these data sources are very useful for natural resource mapping as well as hydrological modelling (Atanaw, 2009).

The influence of evaporation and precipitation on lake water balance is dependent on lake area (Torabi Haghighi & Kløve, 2015a). However, the water balance equation is considered one of the fundamental methods to estimate lake water level fluctuations (Bracht-Flyr et al., 2013; Crapper et al., 1996; Soja et al., 2013). In this study, we will focus on Lake Urmia, one of the largest hypersaline lakes in north-west region of Iran, where anthropogenic effect and natural conditions influence the lake. Fourteen main rivers are contributing in Lake Urmia as inflow sources which play important role to balance lake water volume (Torabi et al., 2018a).

Based on the available dataset and surrounding status of Lake Urmia, in this study we want to focus (I) how different altimeter mission's time series vary to portray water

level for different sections of same lake? We are also interested to know (II) about the status of data accuracy of different observed evaporation stations along with the remote sensing dataset. With the outcomes of altimetry missions we want to identify (III) whether the water level data is deviating from its originality within a specific duration. How other meteorological parameters actually playing role in case of water level response in a lake? Are these enough to define lake performance? To do this, we are going to analyse some scenarios. The main goal is to assess (IV) how well different scenario (combination of field and remote sensing dataset) can explain water balance status within a lake?

1.1 Review of Literature

1.1.1 Water Level and altimetry

Satellite altimetry is a radar technique where measured object feature based on specific principle of functioning (Adam, 2017). The objective of remote sensing tools is to measure the actual distance from satellite orbit for inland water bodies by using a retroreflective radar signal (Bronner et al., 2016). It is also able to acquire climate, environmental phenomena and ocean changes information. For instance, in 1978 sea-sat (Oceanography satellite), in 1985 Geosat (Geophysical satellite and in 1991) ERS1 (European remote sensing satellite) was launched in order to measure the ocean surface topography evidence (Adam, 2017). For different hydrological studies, different innovative satellite missions were launched (e.g. Jason-2, Jason-3, SARAL/Altika, Cryosat-2 and Sentinel-3). Each altimeter mission was placed at a specific gravity position (e.g. latitude and longitude ranges), to receive earth object data through emitted retroreflective wave signal. The obtained emitted wave signal presents specific object source information and is reflected again to satellite data stations. Elapsed datum object in between transmissions and obtained retroreflective radar signal, is proportional to the altitude of the satellite altimetry (Adam, 2017).

Radar altimeter waveform emits electromagnetic pulse to acquire object and reflecting echo recorded into the altimeter (Esa, 2007). Accurate measurement of transit time estimate altimeter ranges from the instrument to the surface. Hence, the range measurement equation can be written as (AVISO, 2017):

$$SH = SA - MR - Co \qquad (1)$$

Where SH represents Surface Height, SA means Satellite Altitude, MR shows Measurement Range and Co is the required Correction.

$$SLA = SSH - MSS \qquad (2)$$

Where SLA refers Sea Level Anomaly, SSH means Sea Surface Height, MSS described Mean Sea Surface. The formula referred above represent variations of altimeter measurement, in between altitude height from above reference ellipsoid to cm accuracy (ESA, 2007). Therefore, by subtracting the range altitude from the measurement range, surface height can be estimated above the reference ellipsoid (Figure 1).
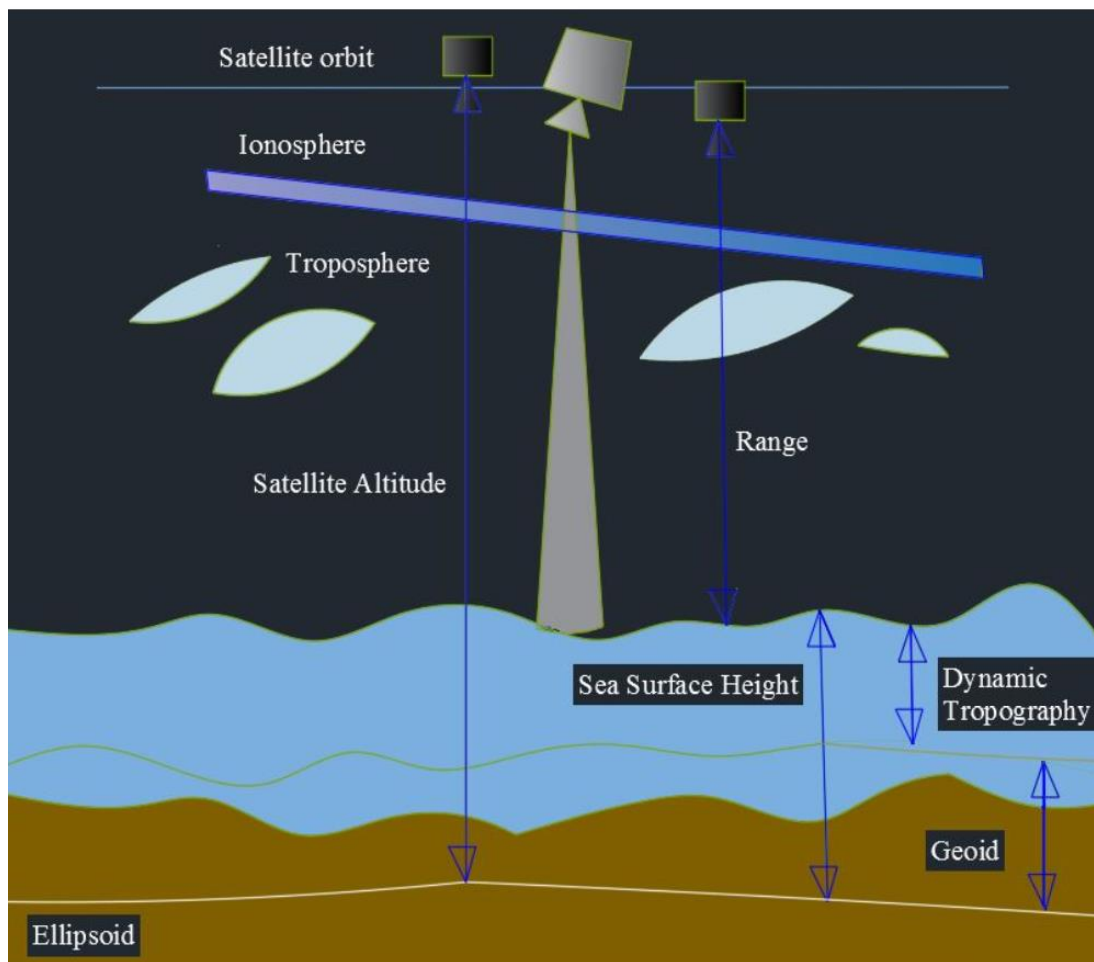

Figure 1. Water Level measurement principle from satellite missions (Sui et al., 2017)

Satellite altimetry track is a communication method between spaceflights and satellite (AVISO, 2017). According to (AVISO, 2017) satellite mission's specification, altimetry

orbits complete a full rotation, from one existing point of latitude to maximum latitude, except for specific difference for odd and even pass number directions. Elliptical mission complete revolution above earth surface through specific periods e.g. 10, 29, 35 or more days. Moreover, each mission contains one unique pass number that varies with earth places. To estimate accurate earth object's data from satellite altimetry sources; instrumentation errors, wet tropospheric effects, dry tropospheric effects, tide influence (earth and pole tide) and atmospheric pressure need to be considered (Mercier et al., 2010).

1.1.2 Evaporation and estimation methods

Evaporation is when liquid transforms into vapour through the change of conditions. It transfers the water from the ocean, inland water bodies, and other water sources into the atmosphere. The vaporization of ocean water always interpreted as the initial stage of hydrological cycle. Above 85% of evaporation occurs in oceans (Mehta et al., 2005). Evaporation occurred into the lake and river basins in different ways. The land surface evaporation is known as evapotranspiration, which includes various components like soil evaporation, transpiration, interception loss, and sublimation. In transpiration process water extracted from vegetation roots also evaporates, in presence of stomatal cells of the leaves. Soil evaporation occurs at top layers of bare soils. The interception loss refers vaporization of the water obtained from the vegetation surface during precipitation. Sublimation occurs when ice and snowpack directly evaporates to the atmosphere.

According to different aspects of hydrological discipline, there are several methods that can be used to estimate evaporation which include (Dingman S.L., 2002); (i) Water-balance approach (ii) Mass-transfer approach (iii) Eddy-correlation approach (iv) Energy-balance approach (v) Penman or combination approach and (vi) Pan-evaporation approach.

The lake surface evaporation process is calculated through energy and water budgets. Land surface energy balance method considers the entire amount of energy is preserved within the system, while energy may transform from one object to another. For instance, net energy radiation (Rn) of land transforms to other forms such as sensible heat (H), ground heat (G) and latent heat fluxes (LE) as equation (3).

$$Rn = H + G + LE \qquad (3)$$

Due to the effect of CO_2 flux on energy balance, the resulting equation forms as,

$$LE = Rn - H - G \qquad (4)$$

Remote sensing platform receives the object information from the earth surface, by emitting electromagnetic radiation. The launched satellite missions of multi-scale database are now extending for further various research possibilities. Wide ranges of accessible data sources are capable to assess evaporation fluctuations. There are several number of remote sensing methods have been developed to assess actual evaporation from satellite sources.

New parameterized method like Simplified Surface Energy Balance (SSEB) and Operational Simplified Surface Energy Balance (SSEBop) are enhancing the scope to estimate evaporation. The Simplified Surface Energy Balance method (SSEB) was developed by (Senay et al., 2007a). This was first executed to thermal data based on uniform agro-hydrologic regions (like an irrigation basin) to assess the impact of elevation and latitude for spatial distribution of evaporation fractions. (Senay et al., 2011b) revised SSEB model to consider the effect of elevation and latitude from the land surface temperature (LST; Ta) and air temperature (Ts). As a result, to estimate evaporation fractions the only remaining requirement was to differentiate air temperature for remote sensing data with identified boundary conditions for hot and cold region (Senay et al., 2013c).

In 2013 the model has been modified from SSEB theory by (Senay et al., 2013c) and others. They developed a new parameterization version of Operational Simplified Surface Energy Balance model (SSEBop) (Su, 2002). This SSEBop model is enable to assess the energy balance terms of each different pixel conditions according to 'wet' and 'dry' reference environment. Due to evaporation, fractions always occur with these mentioning limits (e.g., wet and dry) (Su, 2002). The unique factors of SSEBop model also evaluates predefined boundary conditions to each pixel based on 'hot' and 'cold' reference environment (Senay et al., 2013c). SSEBop model is one of the substantial methods due to its accountability of thermal data information (Mcshane et al., 2017).

Moreover, this model has been used in many cases to explain the status of actual evaporation in large water bodies (Senay et al., 2007a).

1.1.3 Water Balance components in a lake

To assess temporal variations of Lake water level, it is important to know how multiple hydrological components play an important role to balance water cycle within the lake. Now-a-days, Lake water areas quantification by using satellite altimeter images are considered as reliable data source (Rokni et al., 2014). Though there are always some dependency for specific thresholds to define accurate water periphery. Also, the conventional methods for measuring earth water surface feature are expensive and have low accuracy. In some cases, researchers developed several specific algorithm to extract boundary information of lake from satellite images based on the temporal pattern. For example, to estimate monthly water level, (Sima & Tajrishy, 2013) developed area volume depth relationship for Lake Urmia.

Outside of evaporation and initial water level, there are some other major components that always need to be addressed. Rainfall and inflow and outflow status of a lake is viable to understand the phenomenon within the lake. It is always better to use observed rainfall though the temporal availability is always in question. Remote sensing data with consideration of cloud condition can be a better alternative these days.

Temporal variability of inflow and outflow status of a lake sometimes contain measurement issues (Ferguson, 1981). With use of evaporation, initial water level, observed rainfall and surface and groundwater inflow; (Torabi Haghighi & Kløve, 2015a) proposed an approach to simulate Lake water level based on water balance equation. This approach is capable to give an overview about the temporal variability of Lake water level with all plausible hydrological components. In this study, we will also apply similar approach with modifications of different scenario combination to understand water balance status within the lake.

2 MATERIALS AND METHODS

In this chapter, firstly we will focus on study location, available data such as satellite altimetry dataset, DAHITI and different observed dataset. We will also discuss about the detail steps to estimate water level based on combination of multiple data sources including evaporation and rainfall.

2.1 Study area

Lake Urmia is located in northwest of Iran and lies between $37°4'N - 38°17'N$ and $45°13'E - 46°E$, (Figure 2) (Modares, 2018). Lake Urmia was one of the largest hypersaline lakes in Middle East, with maximum surface area of 5000 to 6000 km^2 but present existing area is only 1647 km^2 (Torabi et al., 2018a,Tourian et al., 2015b). In 1971 the Ramsar Convention specified Lake Urmia as a wetland of international importance. This lake was also entitled by UNESCO Biosphere Reserve in 1976 (Nouri et al., 2017). For over a decade, the water volume for Lake Urmia has significantly decreased due to several reasons. Lake Urmia possesses high salinity that goes up to 300 g/L (Eimanifar & Mohebbi, 2007). Compared to typical seawater salinity amount, it is more than eight times (Modares, 2018). More than 6.5 million peoples are dependent on the lake to accomplish their primary source of income (Torabi Haghighi et al., 2018a). Approximately 10% of croplands and orchards occupy lake Urmia's basin area, whereas 90% is consumed by all renewable water resources (Fazel, et al., 2017). Around 75% of inflow water is supplied from surrounding rivers of the lake (Torabi Haghighi et al., 2018a). The main rivers in Lake Urmia basin are Barandoz, Ajichy, Daryan, Gadar, Mahabad, Mahpary, Maedooq, Nazluchay. Qalechay, Shahrchay, Sufichay, Zulachay, Siminehrud, and Zarinehrud (Figure 2).
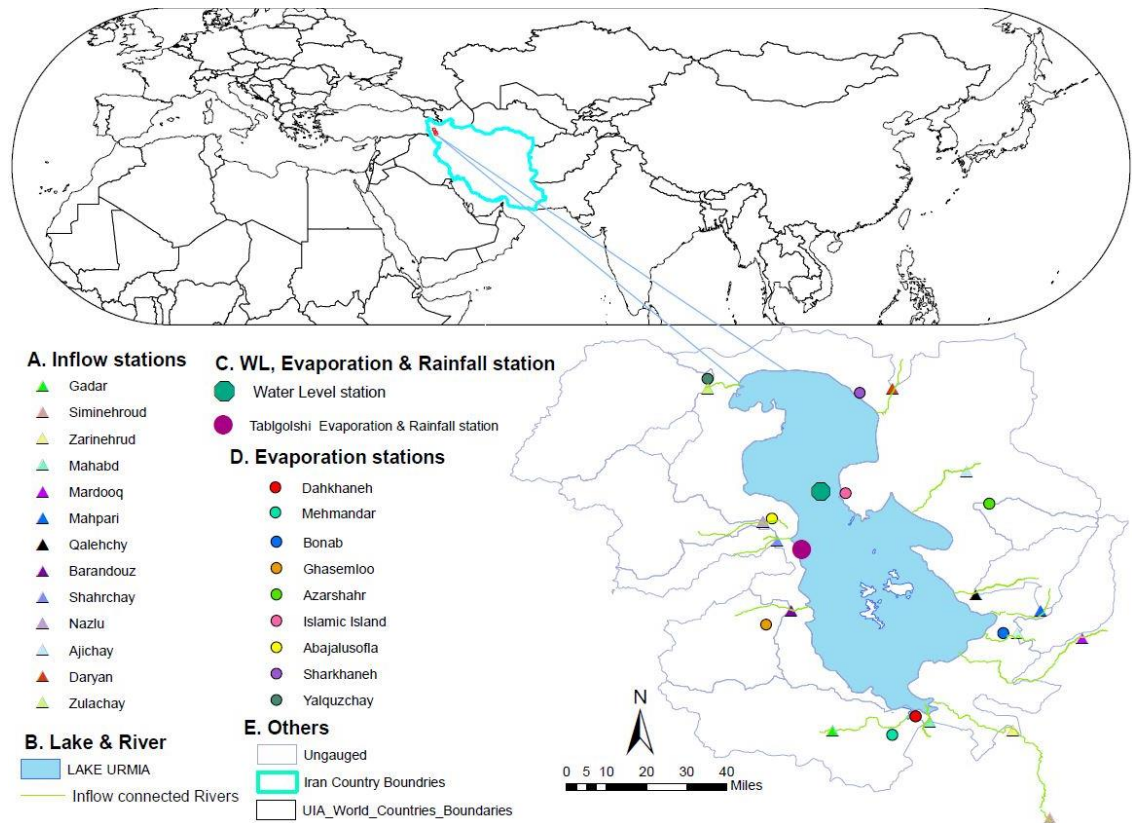
Figure 2. Lake Urmia location with all observed stations

2.1.1 Data collection

Based on (Figure 2), water level station is considered as a source of observed water levels for Lake Urmia. Eleven surrounding stations are taken into account for field evaporation values. Available RS data includes two different satellite altimeter datasets: Jason-2 and Jason-3 for estimating water level variations.

DAHITI and MODIS are considered to retrieve remote sensing water level and evaporation from DAHITI platform (https://dahiti.dgfi.tum.de) and climate engine website (https://app.climateengine.org/) respectively (Table 1).

Table 1. Different satellite missions feature and available time periods

Data type	Data sets	Product	Temporal resolution	Data availability
Observed	WL	x	Daily	2001-2013
	Evaporation	x	Daily	2003-2013
	Inflow	x	Daily	2003-2007
	Rainfall	x	Daily	2003-2007
Remote Sensing	Jason-2	Native GDR-D	9.915~ 10 D	2008-2016
	Jason-3	Native GDR-D	9.915~ 10 D	2016-2018
	MODIS	USGS	1-2 D	1999-active
	DAHITI-WL (Envisat, Jason-1-2-3, Jason-3 (IGDR) Topex/Poseidon)	multi-mission altimetry	multi-mission altimetry	2001-2018

A. JASON-02

Jason-02 mission was launched in August 2008 as an extended version of Jason-01. This mission was jointly conducted by NASA, French space agency, CNES, NOAA, and EU-ETS by (Dumont et al., 2009a). The primary objective of the mission was to extend the data record, release sea level and inland water bodies' measurement. In this study, Native GDR-D (Geophysical Data Records) data is used to estimate water level variations from 2008-2016 (Table 1). Other formats such as Enhanced GDR and NATIVE IGR (Interim Geophysical Data Records) (https://www.aviso.altimetry.fr) from Aviso+ data service are not considered. Moreover, Jason-2 mission cover Lake Urmia with only one single pass (133) which includes cycle number 001-303 with 10 days temporal resolution (Table 1).

B. JASON-03

Jason-03 satellite mission is an updated version of Jason-02, and it has similar objectives like Jason-2 altimeter mission. It was launched in August 2016, and it provides dataset for inland water bodies with 10 days' temporal resolution (Dumont et al., 2016b). Native GDR dataset is also processed in this study to estimate water level

from 2016 to 2018. Jason-3 altimeter mission also covers Lake Urmia with single pass number like Jason-2 mission (Pass 133 with cycles from 25 to 78) (Table 1).

C. MODIS

MODIS (Moderate Resolution Imaging Spectroradiometer) has two different data orbits, namely Terra and Aqua. Aqua mission passes entire earth in every 1-2 days from south to north (ESA, 2000). Processed evaporation data of Lake Urmia from climate engine website (https://app.climateengine.org/) have been collected as climate engine does not contain raw dataset. Climate engine always uses Goole earth's engine platform on their web-browser and process various remote sensing dataset with application of different theoretical algorithms.

D. DAHITI Dataset

According to (Schwatke et al., 2016b), the Database for Hydrological Time Series of Inland Water (DAHITI) was developed to estimate water levels fluctuations of different lakes, reservoirs, rivers, and wetland; based on multi-mission's satellite altimetry. DAHTI database was developed in 2013 by Deutsches Geodätisches Forschungsinstitut Technische Universität München (DGFI-TUM). Based on the availability of multi-missions satellite altimetry it provides extended high temporal resolution dataset in between 10-35 days from 1992. Moreover, estimated results were compared with different observed datasets (https://dahiti.dgfi.tum.de).

E. Climate Engine Dataset

Climate engine was developed in April 2016 to process dataset for spatial and temporal analyses of different remote sensing and gridded meteorological database (https://app.climateengine.org/). Climate engine platform also provides access to download required maps and data time series along with data processing. Moreover, selected region maps and data time series are available in multiple formats in the web link for further processing.

F. Inflow Dataset

Barandoz, Ajichy, Daryan, Gadar, Mahabad, Mahpary, Maedooq, Nazluchay, Qalechay, Shahrchay, Sufichay, Zulachay, Siminehrud, and Zarinehrud are the main contributing rivers in Lake Urmia as inflow sources (Figure 2). Based on the temporal availability of inflow dataset (Figure 6); Siminehrud river is considered as only inflow data source for 2003-2007 for scenario analysis in this study.

G. In Situ Water Level, Rainfall and Evaporation Dataset

In situ water level station (Figure 2) is considered as observed water level data source. Different observed evaporation stations (e.g. Tabgolshi Salty, Tabgolshi Fresh, Mehmandar, Sharafkhaneh, Islamic-Island, Yalquzaqaj, Abajalusofla, Azarshar, Bonab, Dashkhaneh and Ghasemlu) were taken into account to compare with remote sensing data (Figure 2). Based on the statistical outcomes, Tabgolshi Fresh station is chosen for lake water balance simulation (Figure 15 and Table 3); which is also common for observed rainfall (Figure 2).
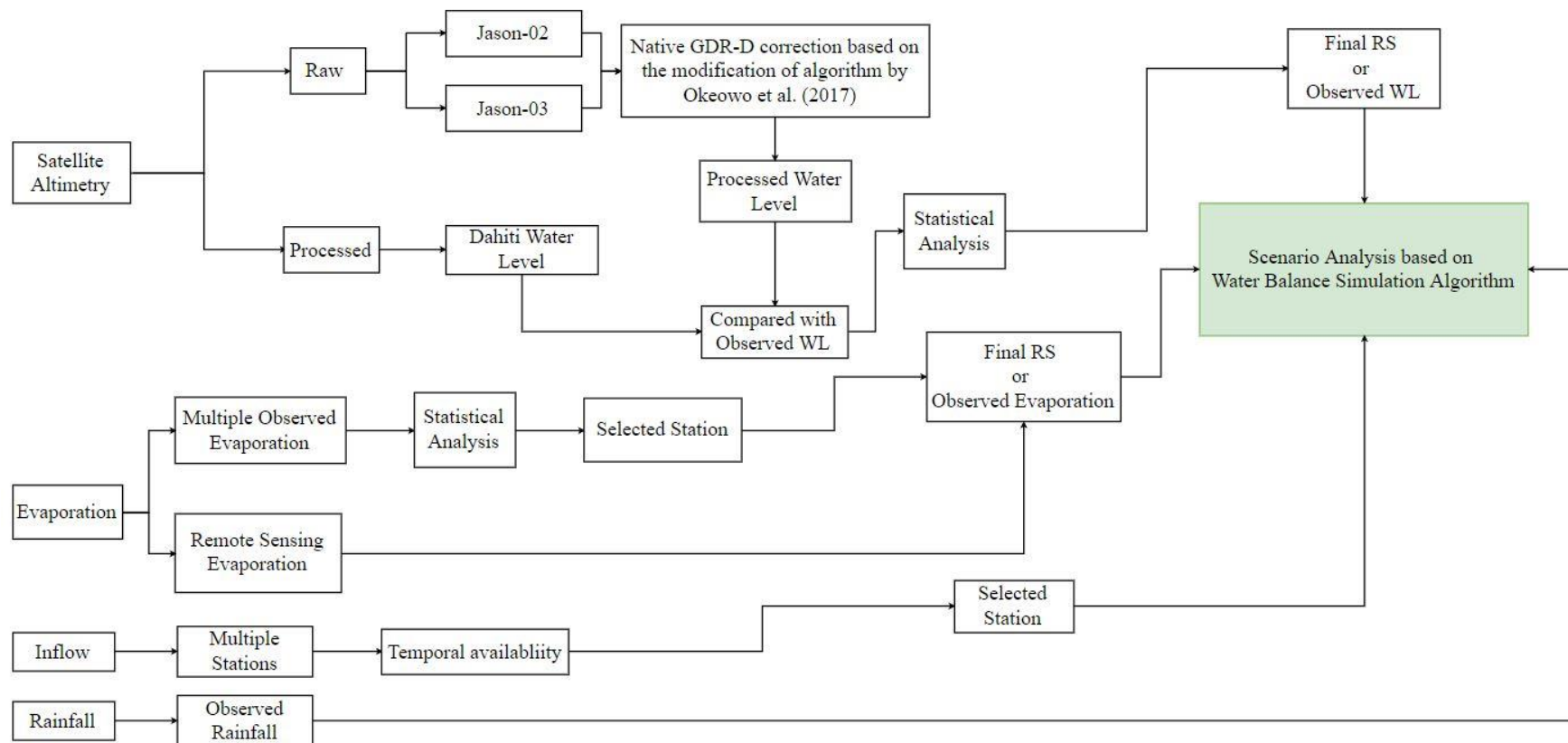
2.2 Methodology

Figure 3. Detail steps to analyze scenario based on all available data sources

In this section, we will mainly discuss about detail steps of water level estimation (Figure 4). We will also focus on evaporation station and inflow station to analyse water balance simulation algorithm (Figure 2).

2.2.1 Water Level estimation from Altimetry mission

   A. Range and Geophysical features:

Range and geophysical features of satellite altimetry represent required range values to estimate water level variations from inland water bodies (Chelton et al., 2001). It considers dry tropospheric correction, wet tropospheric correction and ionospheric correction (Dumont et al., 2009a); which can be written as,

$$CR = R + WTC + DTC + IC \qquad (6)$$

Where CR is Corrected Range, R represents Range, WTC means Wet Troposphere Correction along with DTC (Dry Troposphere Correction) and IC (Ionosphere Correction).

The fundamental range corrections were directed from long distance by satellite radar altimetry tracking. The wet tropospheric correction was important to correct because of the presence of water vapour and cloud liquid of wet droplets (Dubey et al., 2015). These ingredients contribute to slow extension velocity of a radio pulse (Chelton et al., 2001, Mercier et al., 2010, Dumont et al., 2009a). Moreover, earth tide and pole tide are considered the supplementary features of geophysical correction. The corrected geophysical range can be defined as following equation (Dubey et al., 2015),

$$H = Alt - R - [Dtc + Wtc + Ionc + Stc + Ptc] - MSSht \qquad (7)$$

Where, H, Alt and R are the corrected orthometric height, altitude height and satellite range respectively. Dtc, Wtc, Ionc, Stc and Ptc are the dry tropospheric, wet tropospheric, Ionospheric, solid tide and pole corrections sequentially. MSSht is the mean sea surface from the reference ellipsoid.

To estimate water level based on satellite altimetry mission, following steps have been considered (Table 2):

I. Troposphere (Dry and wet): Troposphere considers the lower portion of the atmosphere. When satellite missions of emitted electromagnetic frequency are passing the atmosphere with delay in the travel time, that delay is noted as troposphere (dry and wet) (Hopfield, 1971).

II. Ionosphere: Ionosphere are located into the ionized portion of atmosphere. In this ionized zone free electrons are always present, which is the reason of slow velocity response of electromagnetic frequency (Hopfield, 1971).

III. Pole tide: Pole tide responses to solid earth and the ocean through the centrifugal force because the earth shape is not homogeneous (Desai, 2002, Wahr, 1985).

IV. Saturation: When satellite missions of emitted electromagnetic frequency power differs compared to gain functions of mission's radar receiver (Brenner et al., 2003).

V. Earth Gravitational model is a spherical harmonic expansion model (Lemoine et al., 1998). It defines vertical datum of geodesy, as like as estimating ellipsoid height differences. EGM96 geoid originated from EGM84 geoid undulation model. With collaboration of 'The National Imagery and Mapping Agency (NIMA), The Ohio State University (OSU) and The NASA Goddard Flight Centre (GSFC) consider Earth Gravitational potential degree (360) to develop EGM96 model. Moreover, EGM2008 is also a spherical harmonic expansion model to define vertical datum, but major difference from the EGM96 model is the inclusion of GRACE gravity field data (Roman et al., 2010).

Table 2. Range correction feature

Correction	Mission	
	Jason-02	Jason-03
Dry atmosphere	√	√
Wet atmosphere	√	√
Ionosphere	√	√
Solid earth tide	√	√
Pole tide	√	√
Saturation	-	-

B. Steps of Water Level estimations:

In case of Lake Urmia, Lake water level and width are decreasing. It is difficult to estimate water level without correcting the errors (Schwatke et al., 2015a). In order to avoid errors and ensure better water level assessment, the lake is divided into three sections based on Jason-2 and Jason-3 altimeter crossing passes (section 3.1).

To estimate water level from satellite altimetry, correction parameters are modified as described in (see A) based on the developed algorithm by (Okeowo et al., 2017). Following steps have been considered to semi-automate the process of estimating water level from Jason-02 and Jason-03 missions (Figure 4).
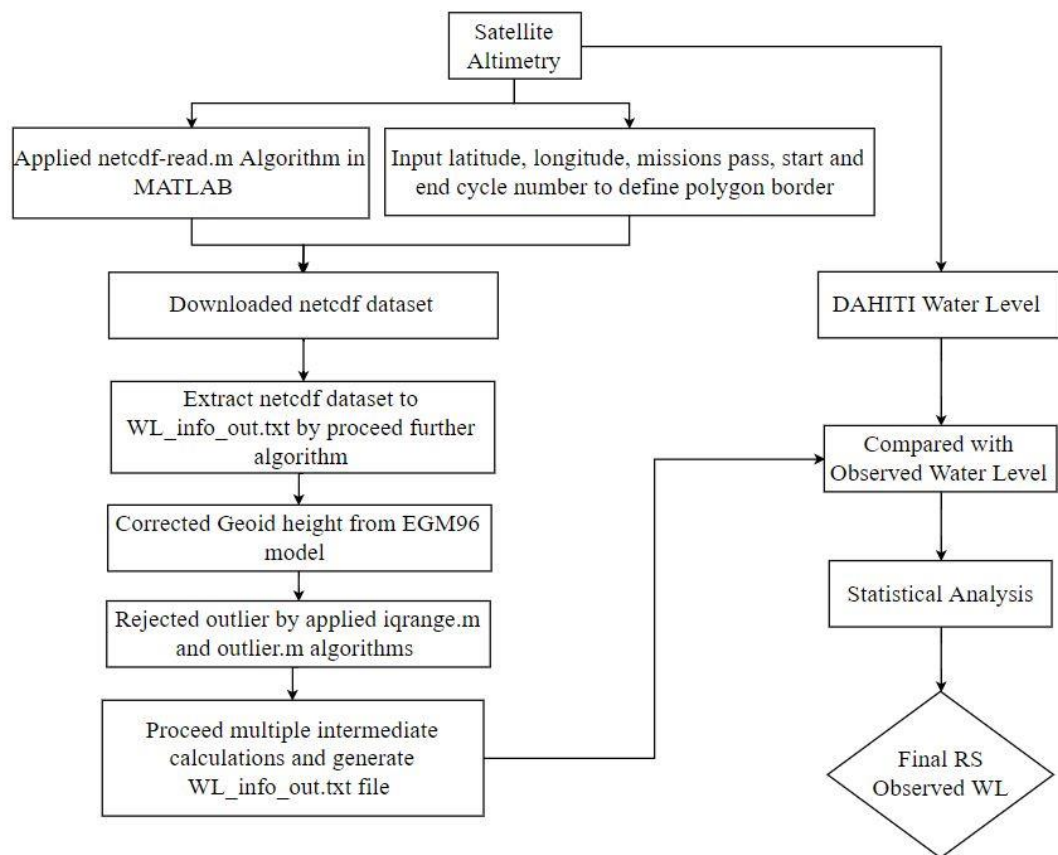

Figure 4. Steps of Water Level estimation process.

I. Different locations (e.g. East, East-b and South) of Lake Urmia have been selected where Jason-2 and Jason-3 satellite missions cover lake area from AVISO+ online data extraction service (https://www.aviso.altimetry.fr). A polygon is defined over the altimeter pass.

II. To read the data sources based on the developed algorithms by (Okeowo et al., 2017), netcdf_read.m is used in MATLAB. It provides latitude and longitude, altimeter missions pass, start and end cycle's number that are inside the polygon border. Raw data set in netcdf format is downloaded from Aviso+ website.

III. Further algorithms are also applied to extract netcdf dataset to water level (WL_info_out.txt). Multiple intermediate calculations (extract.m) have been considered to generate WL_info_out. txt file. By using iqrange.m and outlier.m files, outlier is corrected. Geoid height is also modified by using EGM96 model instead of EGM08 (see A)

IV. At this stage, the final estimated water level have been estimated from satellite altimetry after having the correction from Geoid height. The algorithm worked in a way that it can plot water level time series from the specific mission.

Using the above approach (Figure 4), water levels for multiple locations of Lake Urmia are estimated (Figure 8 and Figure 11). Comparison is also taken into account for observed and DAHITI dataset with estimated water level, which are given in results section (Figure 9).

2.2.2 Evaporation

Estimated evaporation of Lake Urmia from Climate engine (Abatzoglou & Hegewis, 2016) are considered where they used Operational Simplified Surface Energy Balance (SSEBop) model approach (https://app.climateengine.org/). Estimated remote sensing evaporation stations from lake surrounding area were selected to identify most reliable station for further analysis. The detail steps of application of Simplified Surface Energy Balance (SSEBop) is described below (Figure 5).
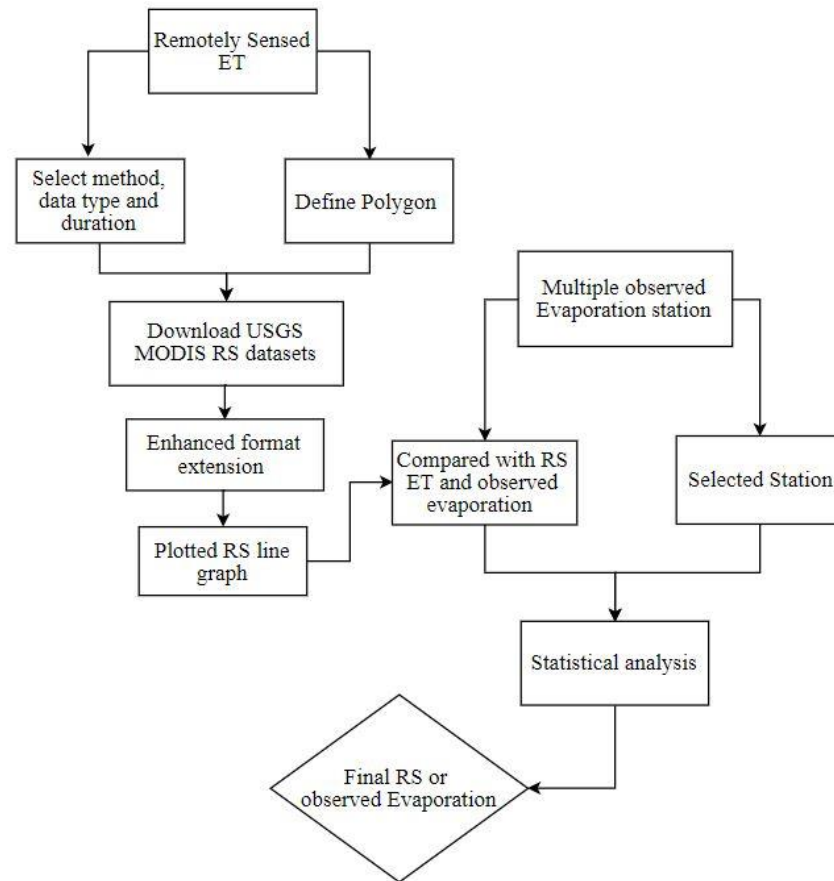
Figure 5. Steps to use evaporation data from Climate engine (Abatzoglou & Hegewisch, 2016)

I.   As a first step, a polygon is defined over the lake area using climate engine service to download daily evaporation data from 2003 to 2007.

II. Monthly ratio has been estimated between each observed station's data and remote sensing data. One specific station for further analysis is identified based on the outcomes of the ratio. One of the main reasons to do this monthly ratio analysis is to assess the monthly variability between pan evaporation from the field and evapotranspiration from remote sensing dataset (Figure 15 and Table 3).

III. Multiple line graphs are plotted to compare between climate engine dataset and observed evaporation (Figure 13). Eleven different observed evaporation stations are considered from lake surrounding area (Figure 15 and Table 3). Based on statistical analysis and temporal availability (section 3.2), Tabgolshi fresh station is only chosen for further analysis (Figure 14 and Figure 15).

2.2.3 Water Balance Simulation

At this stage, we have observed water level from in situ water level station (Figure 2) and remote sensing water level from DAHITI platform (https://dahiti.dgfi.tum.de). In case of evaporation, we have both field and remote sensing dataset.

To begin with, one of the most effective methods is to assess water balance simulation to get status about storage and water level of the lake (Bracht-Flyr et al., 2013; Crapper et al., 1996; Morrill et al., 2001; Soja et al., 2013; Tsubo et al., 2007). We considered a MATLAB script developed by (Torabi Haghighi & Kløve, 2015a), which operates based on the following equation of lake water balance:

$$V_{i+1} - V_i \text{ (Storage)} = \left(\text{inflow} \left(\sum Q_I \right) - \text{outflow} \left(\sum Q_o \right) \right)_i \qquad (8)$$

We considered all the available dataset on a monthly basis. The above equation calculates amount of water stored in a month within the lake based on the amount of inflow and outflow of the lake. For inflow, we considered (Figure 2) rainfall and (Figure 6) inflow stations to apply in water balance equation. (Figure 6) represents the available period of inflow data from surrounding rivers around Lake Urmia. Out of all available stations, we used Siminiehrud station in this study.
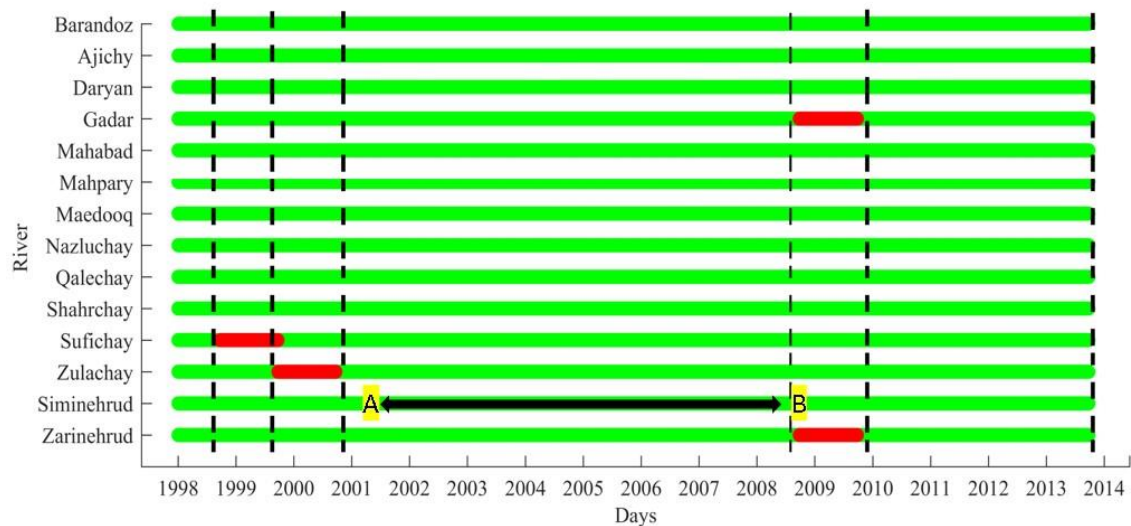

Figure 6. Availability of inflow dataset from surrounding rivers.

We considered evaporation as the only source of outflow for the lake within a specific month. To estimate water level at the end of the month, we used area volume depth relationship developed by (Sima & Tajrishy, 2013) for Lake Urmia.

Based on different input data sources in equation (8), we considered four different scenarios for Lake Urmia to assess water balance status (Figure 7). We used combination of remote sensing and observed dataset in different scenarios such as water level, evaporation and rainfall (Figure 16).
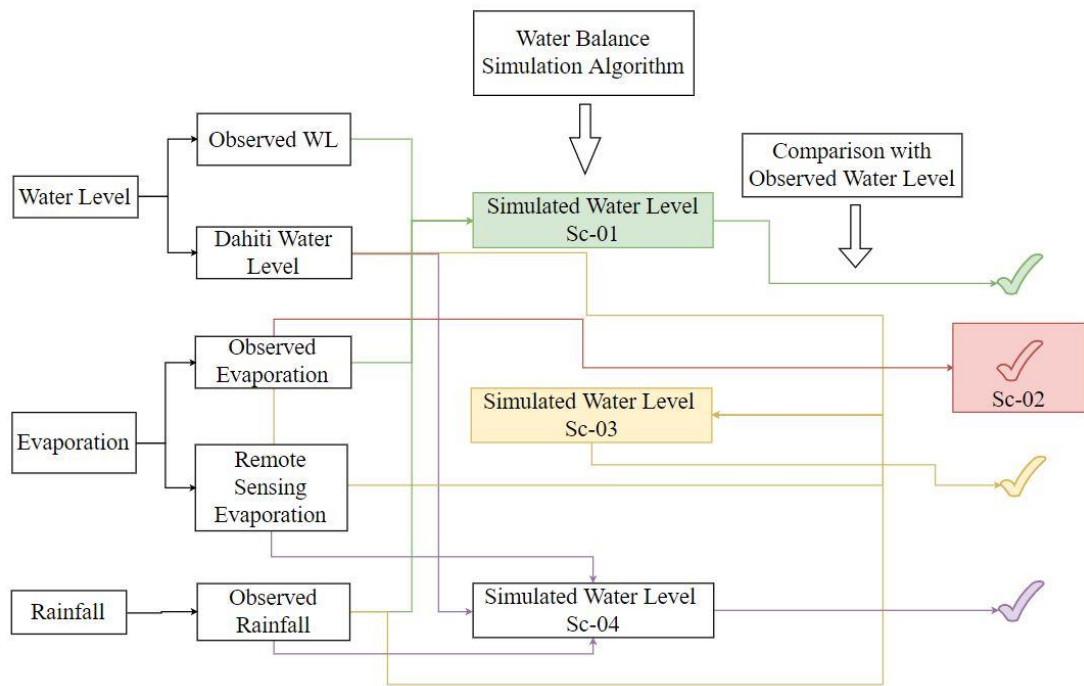

Figure 7. Different water level scenarios based on combination of multiple sources.

We also considered statistical analysis between each simulated water level and field water level. In this study, we used scatterplot to focus how data points are varying with each other from both sources (section 3). We calculated correlation coefficient that is noted as a statistical measurement to define the strength of relationship between two variables. It also shows how strongly pairs of each variables are related.

3 RESULTS

3.1 Lake Urmia water level: RS and observed data:

The Urmia lake water level fluctuation (WLF) was estimated based on two altimeter missions: Jason-02 for 2008-2016 and Jason-03 for 2016-2018. The WLF for three sections of Lake Urmia which are covered by J2-J133 and J3-J133 paths, were estimated and compared with observed and DAHITI data.

3.1.1 Lake Urmia WLF based on Jason 2

The estimated water level shows well pattern after 2010-2013 period as compared with observed and DAHITI data. Observed data shows a higher WLF (Figure 8.a). For example, from 2008-2010 the difference in the water level was around 0.97 m whereas it was slightly lower from 2011 to 2013 (about 0.4 m). However, estimated results from DAHITI show a similar pattern of WLF, like observed data. For instance, from 2008-2010 the difference in the water level was around 0.74 m, from 2010-2016 the difference was gradually decreased to 0.45 m. It is also visible that the estimated WLF for the lake was higher for first section, compared to observed data.

According to second section, from July 2009 to 2013, estimated results show considerably lower WLF compared to observed data, and difference was about 0.29 m. While in June 2008-2009 the WLF was partially higher (average 0.41 m) (Figure 8.b). In contrast, for DAHITI data, from August 2008-2009, estimated WLF was lower and well agreed and difference in the water level was about 0.12 m. In November 2009-2010, result shows several higher and lower WLF around 0.33 m. From 2011-2016 it shows similar pattern of WLF, but the difference was slightly higher with an average of 0.40 m, compared to earlier 2009-2010 period. Compared to the results of first section (Figure 8.a), (Figure 8.b) shows that the water level was fluctuated to a certain extent in the selected second section of the lake.
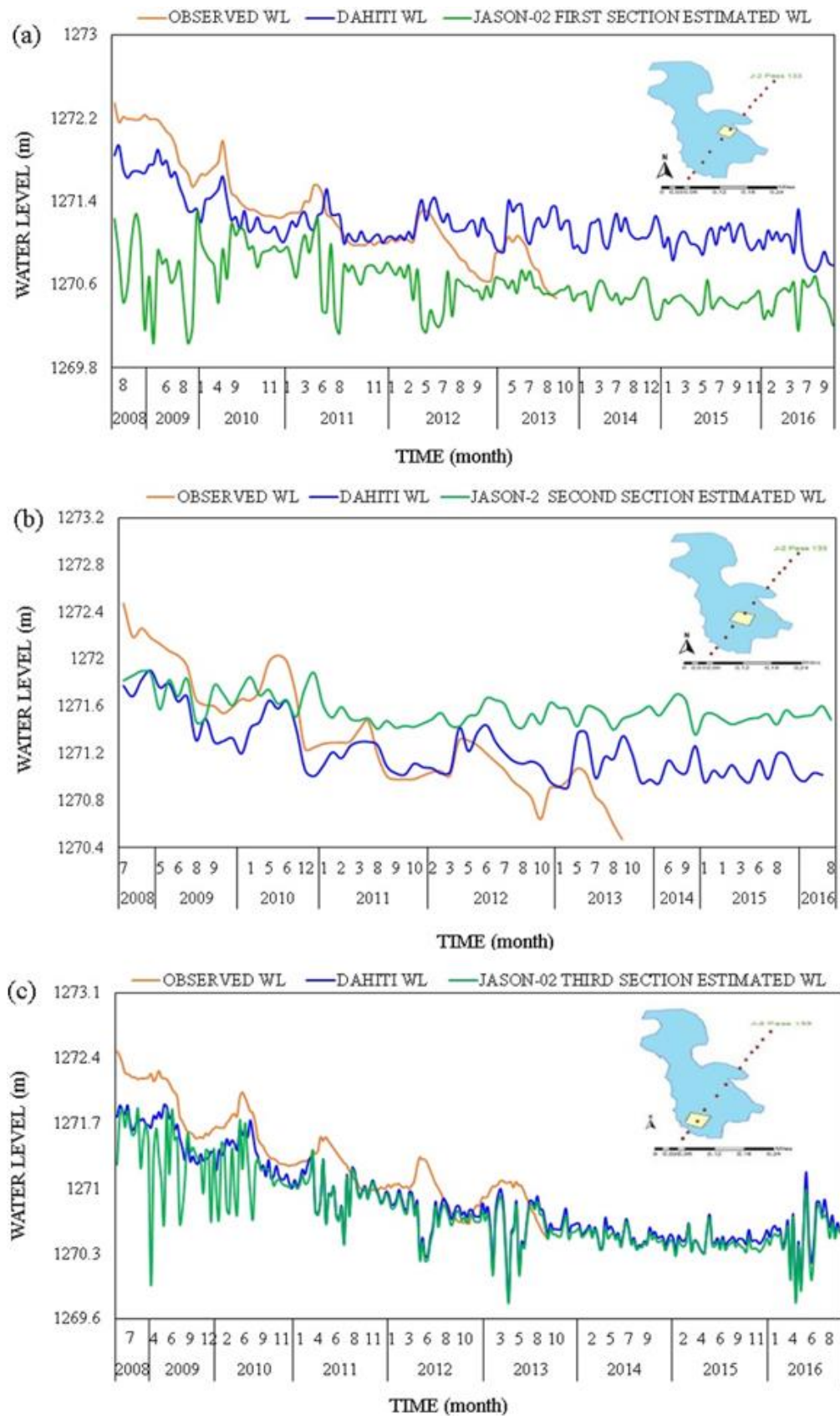
Figure 8. Comparison of monthly observed and DAHITI water level fluctuation at Lake Urmia with the estimated water level based on Jason-2 altimetry mission in a) First section b) Second section and c) Third section.

Estimated WLF in third section are not well agreed with observed data (Figure 8.c). The estimated WLF shows well pattern from 2010-2013 period. The difference in the water level between the estimated results and the observed data for the initial period in 2008 was higher and found to be around 0.67 m (Figure 8.c). From 2009-2013, each year shows several higher and lower WLF. From 2009-2010 result shows higher WLF around 0.62 m and 0.46 m respectively whereas it was an average of 0.29 m, 0.28 m and 0.38 m for the year of 2011, 2012 and 2013.

On the other hand, from 2008-2012 estimated results shows higher WLF with DAHITI data and average difference in the water level for each year was about 0.18 m, 0.32 m, 0.24 m, 0.03 m and 0.05 m, respectively. Moreover, from 2013-2016, result shows substantial lower WLF and average difference in the water level for each year was around 0.06 m, 0.03 m, 0.05 m and 0.07 m respectively.

To assess the results of Jason-2 estimated WLF, statistical analysis was also conducted to compare between observed and DAHITI data where it shows positive correlation ($R^2 = 0.96$, Figure 9).
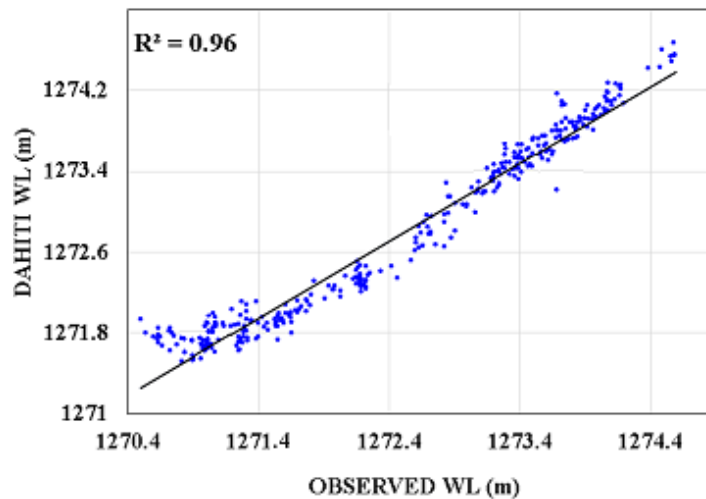

Figure 9. Correlation coefficient between. Observed and DAHITI datasets.

The estimated WLF for section one didn't show well correlation with observed data ($R^2 = 0.10$, Figure 10.a). In case of DAHITI, the correlation is very poor ($R^2 = 0.04$, Figure 10.b). The estimated WLF for section two shows comparatively better correlation with observed data than first section ($R^2 = 0.42$, Figure 10.c). For DAHITI data, results show partially worse correlation ($R^2 = 0.27$, Figure 10.d), compared to earlier results ($R^2 =$

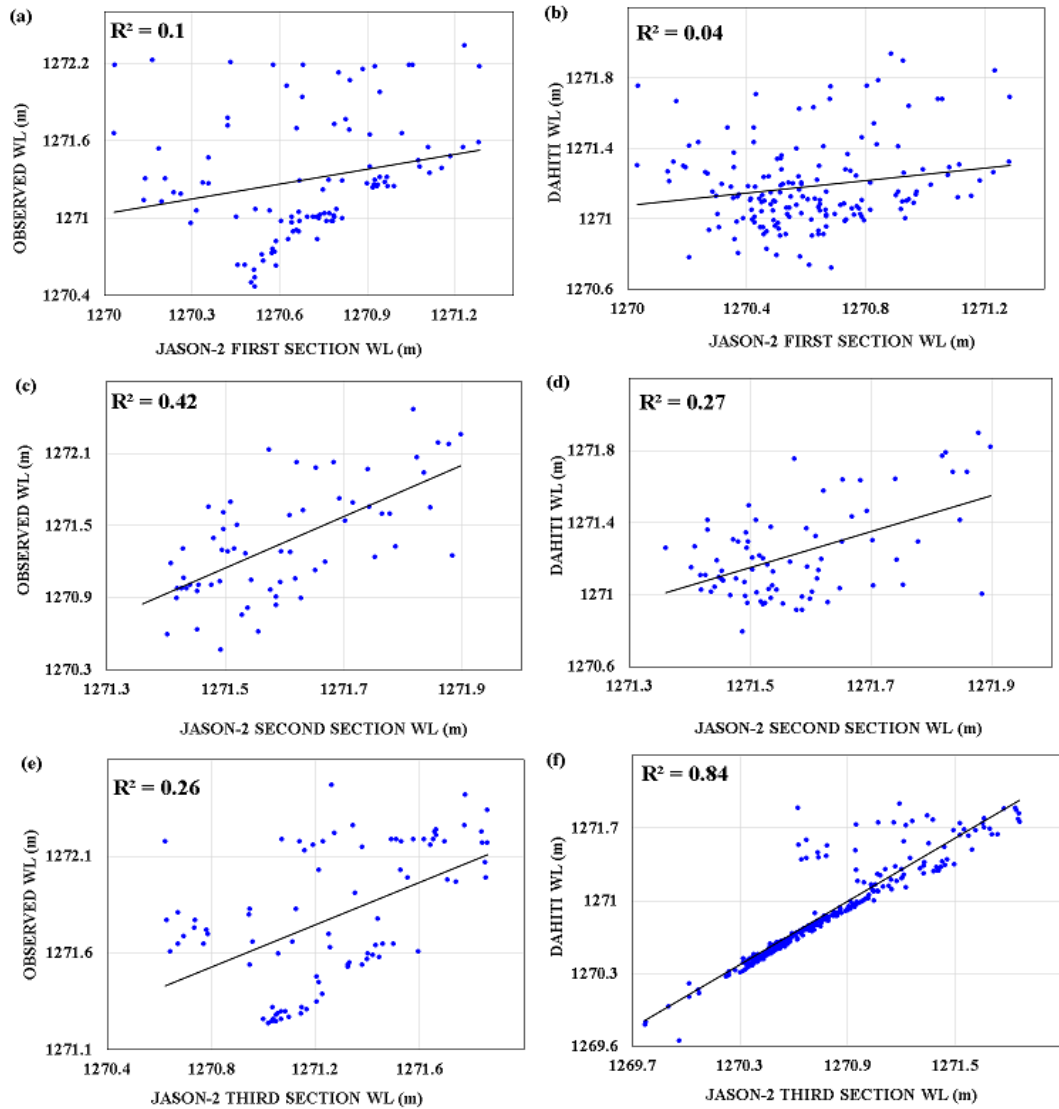0.42, Figure 10.c). Finally, the estimated results for second section show well pattern than section one.

Figure 10. Estimated, Observed and DAHITI data sets correlation coefficient for Jason-2 altimetry. (a) First section vs observed (b) First section vs DAHITI. (c) Second section vs observed. (d) Second section vs DAHITI. (e) Third section vs observed. (f) Third section vs DAHITI.

According to the (Figure 10.e, f), where the third section of the lake was compared to observed data results did not show well correlation ($R^2 = 0.26$, Figure 10.e). But for DAHITI it shows considerable correlation ($R^2 = 0.84$, Figure 10.f). As a result, the third section of the lake based on Jason-2 altimetry also shows substantial accuracy of WLF when DAHITI data is considered.

3.1.2 Lake Urmia WLF based on Jason 3

The first section of estimated result showed a poor pattern of the WLF from 2016 to 2017 period with DAHITI data. The estimated results displayed higher WLF from June-October 2016 with an average of 0.35 m (Figure 11.a). From November 2016 to February 2017, WLF gradually decreased around 0.12 m. From March 2017 to 2018 result showed partially similar pattern of WLF like 2016-2017 period. In April 2018, WLF was considerably decreased to 0.45 m average, though between May-August it showed higher WLF and difference in the water level was around 0.87 m.

The second section of estimated results from 2016-2017 showed dynamic consistency of WLF and minimum difference in the water level was around 0.01 m, except for month of May when the difference was around 0.20 m (Figure 11.b). From November 2016 to June 2017 the WLF was considerably lower (average 0.08 m), between July-August 2017 it showed similar pattern of lower WLF. From July-December the WLF was partially higher (approximately 0.11 m). In 2018 result showed maximum amplitude of difference in the water level as compared to 2016 - 2017 period.

Estimated results in third section showed several higher and lower WLF from 2016-2018 period (Figure 11.c). For example, from October-December 2016 the WLF was partially lower and the difference in the water level was around 0.14 m. In 2017, from January-April it showed WLF of around 0.12 m, from May-December the value was around 0.34 m. In 2018, from January-May it showed maximum amplitude of WLF. Estimated results in third section showed higher WLF compared to earlier two sections (Figure 11.a, b).
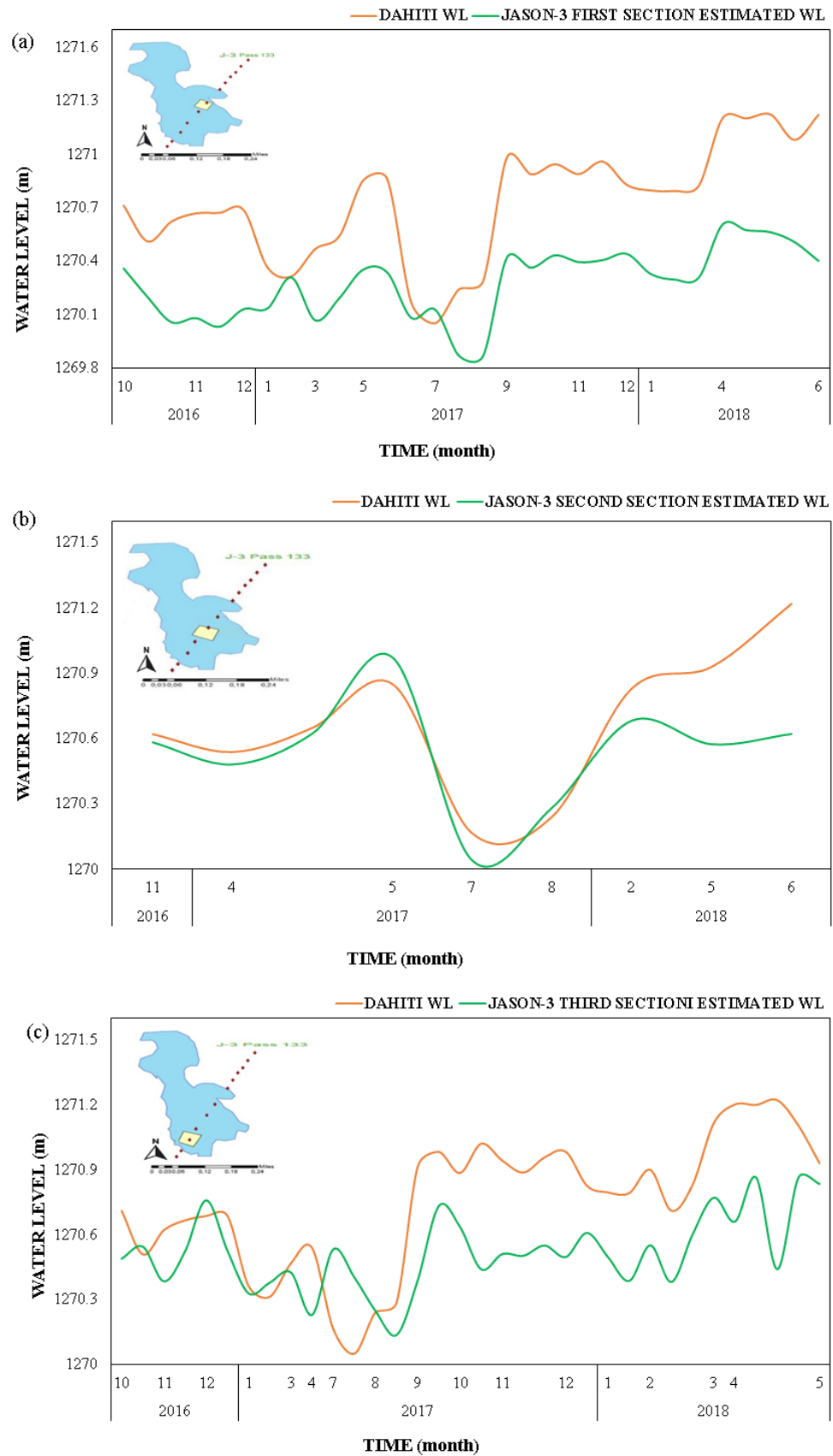
Figure 11. Comparison between monthly observed water level fluctuations with estimated water level at Lake Urmia based on Jason-3 altimetry missions in a) First section b) Second section c) Third section.

To validate the results of Jason-3 estimated WLF statistical analysis was performed with DAHITI data. The estimated WLF in section one showed considerably well correlation with DAHITI data (R^2 = 0.69, Figure 12.a). While, estimated WLF in second section showed slightly poor correlation (R^2 = 0.56, Figure 12.b). In section three it showed very poor correlation (R^2 = 0.37, Figure 12.c) which is quite worse rather than earlier two results (Figure 12.a-b). Moreover, the statistical analysis did not show any worthy linear regression for Jason-3 (Figure 12) but explained well consistent correlation as compared to earlier results of Jason-2 altimetry (Figure 10).
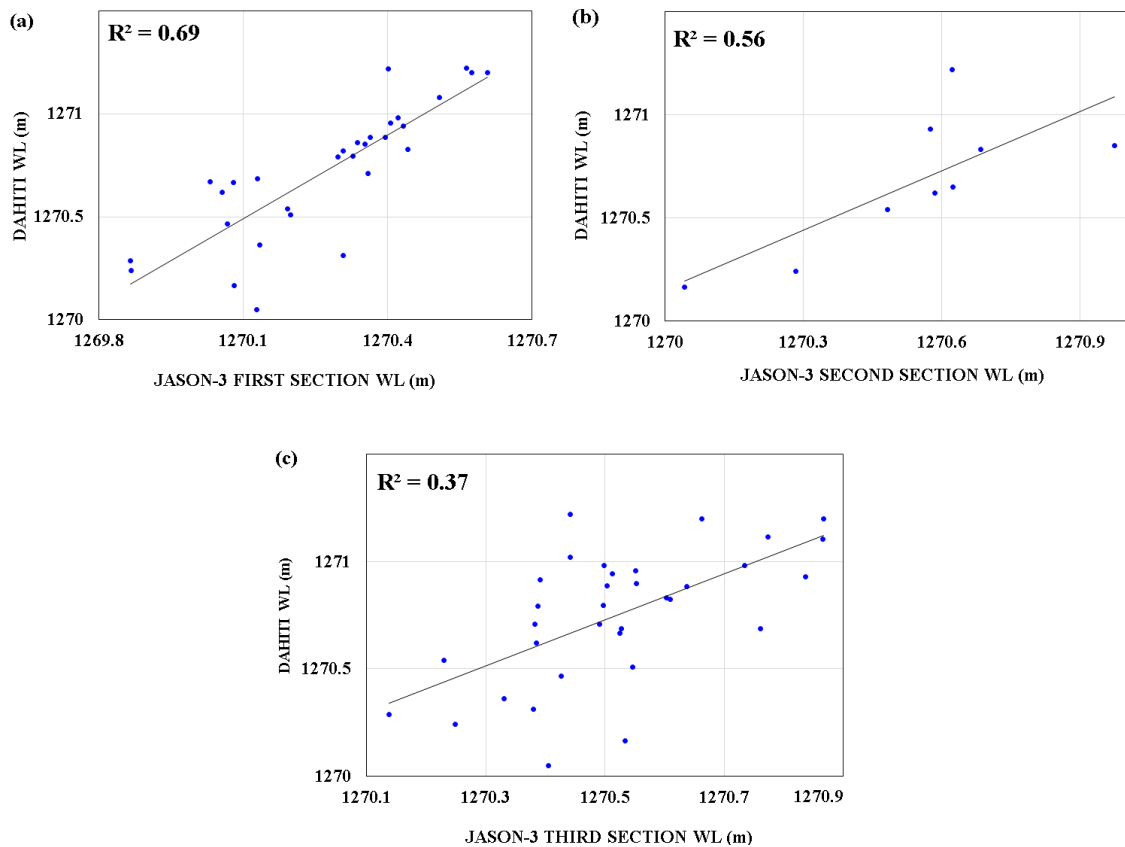

Figure 12. Estimated and DAHITI dataset correlation coefficient for Jason-3 altimetry (a) First section vs DAHITI (b) Second section vs DAHITI. (c) Third vs DAHITI.

Furthermore, according to the statistical analysis between Jason-2 and Jason-3 estimated WLF results, Jason-2 estimated WLF results showed better estimation particularly for DAHITI data (Figure 10.f).

3.2 Evaporation from Lake Urmia: RS and observed data

Monthly observed evaporation and the results of remote sensing evaporation for 2003-2007 were compared (Figure 13). Monthly and annually observed evaporation was consistent as well as in good agreement with remote sensing evaporation (Figure 13). According to (Figure 13.a) in August 2005 the Islamic-Island observed evaporation showed highest evaporation (approximately 539 mm). Throughout the period from 2003-2013, evaporation during June July was always higher than other months.
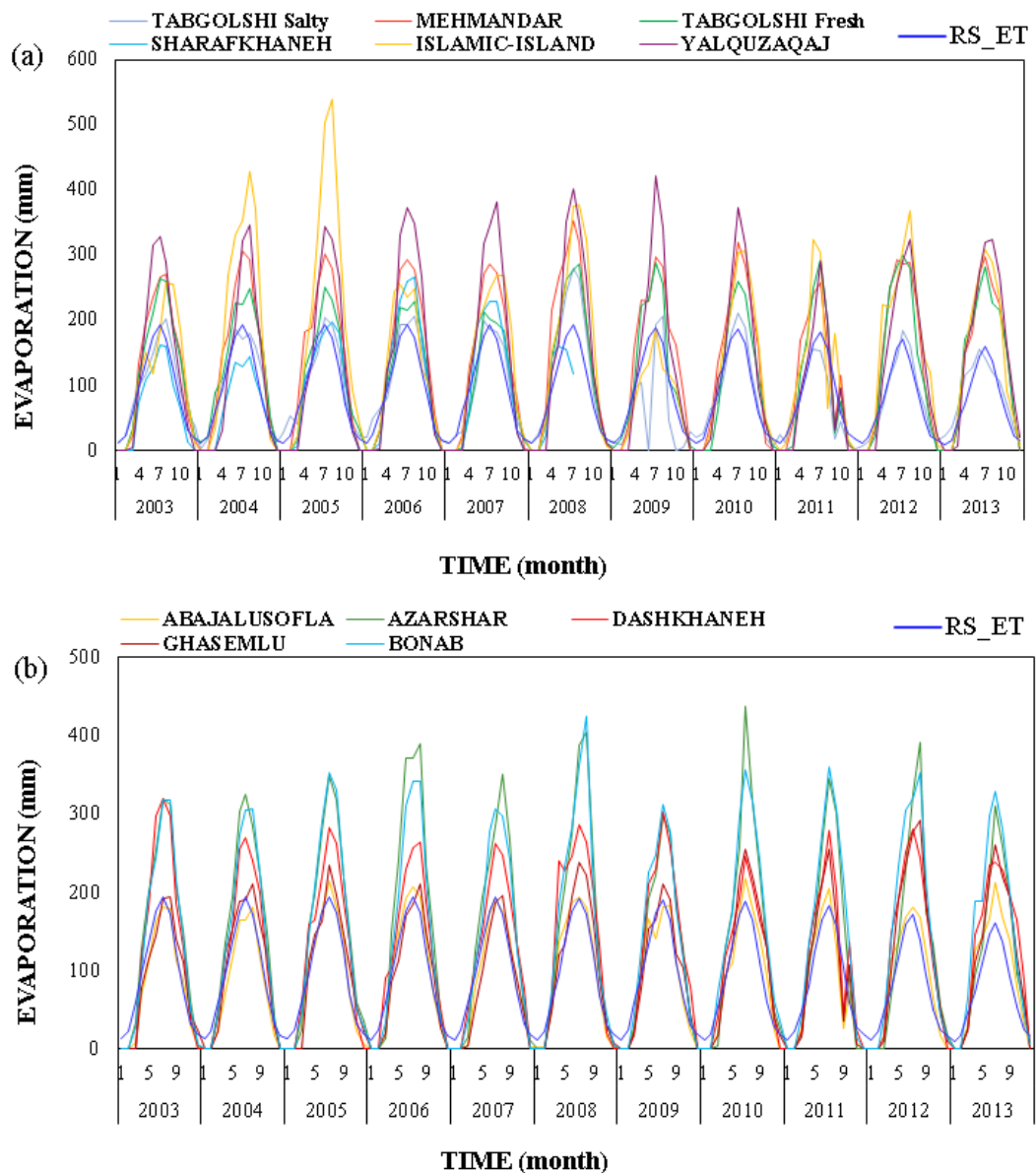

Figure 13. Monthly temporal evaporation of different observed stations and RS. Observed vs RS (a) (Tabgolshi Fresh, Tabgolshi Salty, Islamiclsland, Yalquzaqaj, Sharafkhaneh, Mehmandar) and (b) (Abajalusofla, Azarshar, Dashkhaneh, Ghasemlu, Bonab).

According to (Figure 13.b) in July 2010, Azarshar observed station showed highest evaporation (approximately 437.8 mm) and in August 2008 Bonab station also had high evaporation (425.6 mm). From 2003-2013 period both stations (e.g. Azarshar and Bonab) showed consistently higher evaporation compared to others. RS evaporation always showed consistently low rate of evaporation than all observed evaporation stations (Figure 13.a and Figure 13.b).

All observed evaporation stations are showing well correlation with remotely sensed evaporation (Figure 14). For instance, Bonab and Abajalusofla evaporation stations showed higher correlation coefficient, ($R^2 = 0.93$) and ($R^2 = 0.92$) (Figure 14.k, c), while the other three evaporation stations (Dashkhaneh, Azarshar, and Mehmandar) showed almost similar correlation ($R^2 = 0.90$) (Figure 14.e, d, j).
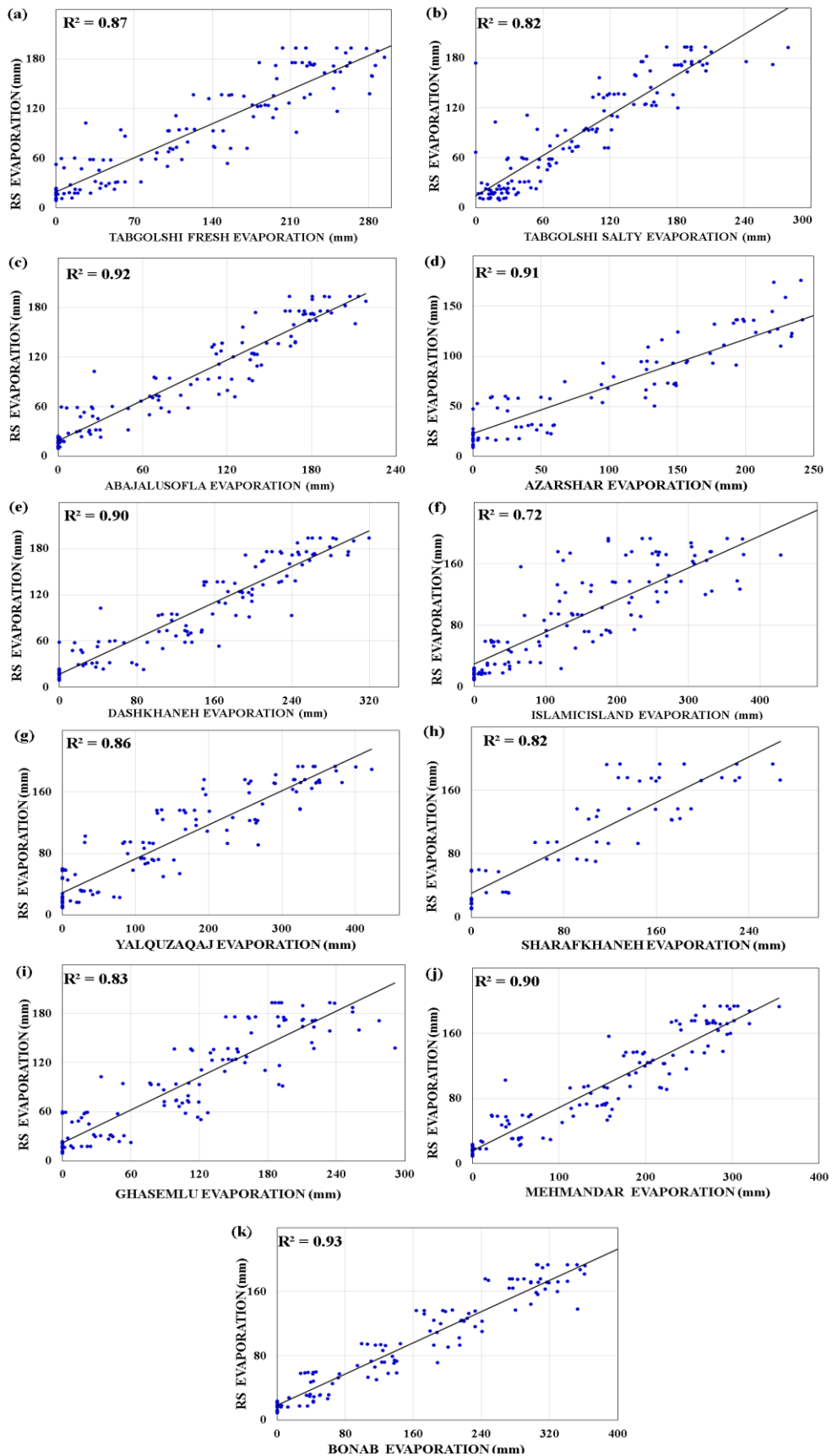
Figure 14. Correlation coefficient in between RS and observed stations (a) Tabgolshi fresh (b) Tabgolshi salty (c) Abajalusofla (d) Azarshar (e) Dashkhaneh (f) Islamiclsland (g) Yalquzaqaj (h) Sharafkhaneh (i) Ghasemlu (j) Mehmandar (k) Bonab.

Some observed evaporation stations showed slightly poor correlation like Tabgolshi fresh ($R^2 = 0.87$), Yalquzaqaz ($R^2 = 0.85$), Tabgolshi salty ($R^2 = 0.83$), Ghasemlu ($R^2 = 0.83$) and Sharafkhanesh ($R^2 = 0.82$) (Figure 14.a, g, b, I and h). Based on statistical correlation Bonab evaporation station has strong agreement with remote sensing data.

In addition, in (Figure 15), all observed evaporation between January-February have the lowest evaporation ratio (around 0.17), except in Tabgolshi SWS where observed evaporation is around 1.20. From March-November the evaporation ratio is continuously increasing with an average of 1.45, compared to all other observed evaporation stations. Though in October the evaporation ratio is highest (around 1.72), and at the end of December, the evaporation ratio has decreased to around 0.36.
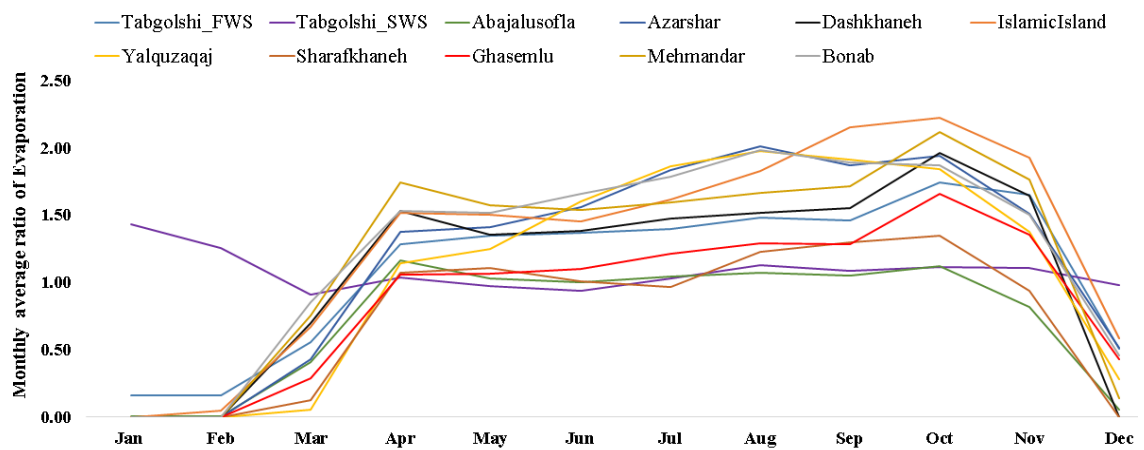
Figure 15. Monthly average ratio of evaporation in between RS data vs. observed data.

Based on the results (Figure 15 and Table 3), it is clear that Tabgolshi fresh evaporation station shows important variations throughout the year. For example, from January to March it shows an average of 0.29 whereas the value is 1.36 from April to December. Because of statistical output (monthly variation of ratio) and location of Tabgolshi fresh station, it was selected for further analysis in this study out of all other stations.

Table 3. Monthly ratio in between observed evaporation and remote sensing data.

Ratio	Months											
IN SITU/RS	1	2	3	4	5	6	7	8	9	10	11	12
Tabgolshi_FWS	0.16	0.16	0.55	1.28	1.35	1.37	1.39	1.48	1.46	1.74	1.65	0.50
Tabgolshi_SWS	1.43	1.26	0.91	1.04	0.97	0.94	1.03	1.13	1.09	1.12	1.10	0.98
Abajalusofla	0.01	0.00	0.41	1.16	1.03	1.00	1.05	1.07	1.05	1.12	0.81	0.05
Azarshar	0.00	0.00	0.43	1.37	1.41	1.56	1.83	2.01	1.87	1.94	1.51	0.51
Dashkhaneh	0.00	0.00	0.70	1.53	1.35	1.38	1.47	1.51	1.55	1.96	1.64	0.00
Islamic-Island	0.00	0.05	0.67	1.51	1.50	1.45	1.62	1.83	2.15	2.22	1.93	0.58
Yalquzaqaj	0.00	0.00	0.05	1.14	1.25	1.60	1.86	1.98	1.91	1.84	1.37	0.28
Sharafkhaneh	0.00	0.00	0.13	1.07	1.11	1.01	0.97	1.23	1.30	1.35	0.94	0.00
Ghasemlu	0.00	0.00	0.29	1.06	1.06	1.10	1.21	1.29	1.28	1.66	1.35	0.43
Mehmandar	0.00	0.00	0.76	1.74	1.57	1.54	1.59	1.66	1.71	2.11	1.77	0.14
Bonab	0.00	0.00	0.86	1.53	1.51	1.66	1.79	1.98	1.89	1.87	1.50	0.46
RS_ET	1.00	1.00	1.00	1.00	1.00	1.00	1.00	1.00	1.00	1.00	1.00	1.00

3.3 Accuracy assessment and Water Balance:

(Figure 16) represents estimated water level with respect to observed water level for four different scenarios for 2003-2007. The simulated water level show lower and slight variations from observed data.

Based on Sc-01 (Figure 16.a) during 2003-2004 the simulated water level was about 0.05 m lower than observed water level and this difference had increased to 0.07 m for 2005-2007 (Figure 16.a).

In case of Sc-02 in 2003, the simulated water level was 0.38 m lower than observed water level and from 2004-2007 it showed higher amplitude (0.43 m) (Figure 16.b). Moreover, it is visible that Sc-02 simulated water level time series did not show well pattern like Sc-01 (Figure 16.a).

In 2003, for Sc-03 the simulated water level was slightly varied with an average of 0.28 m with observed water level and this difference was increased to 0.30 m for 2004. After that, simulated water level difference was increased around 0.34 m from 2005-2007 (Figure 16.c).

Simulated WL based on Sc-04 was around 0.37 m lower than observed water level in 2003 and this difference was gradually fluctuated to 0.32 m, 0.28 m, 0.30 and 0.32 m respectively from 2004 to 2007 (Figure 16.d).
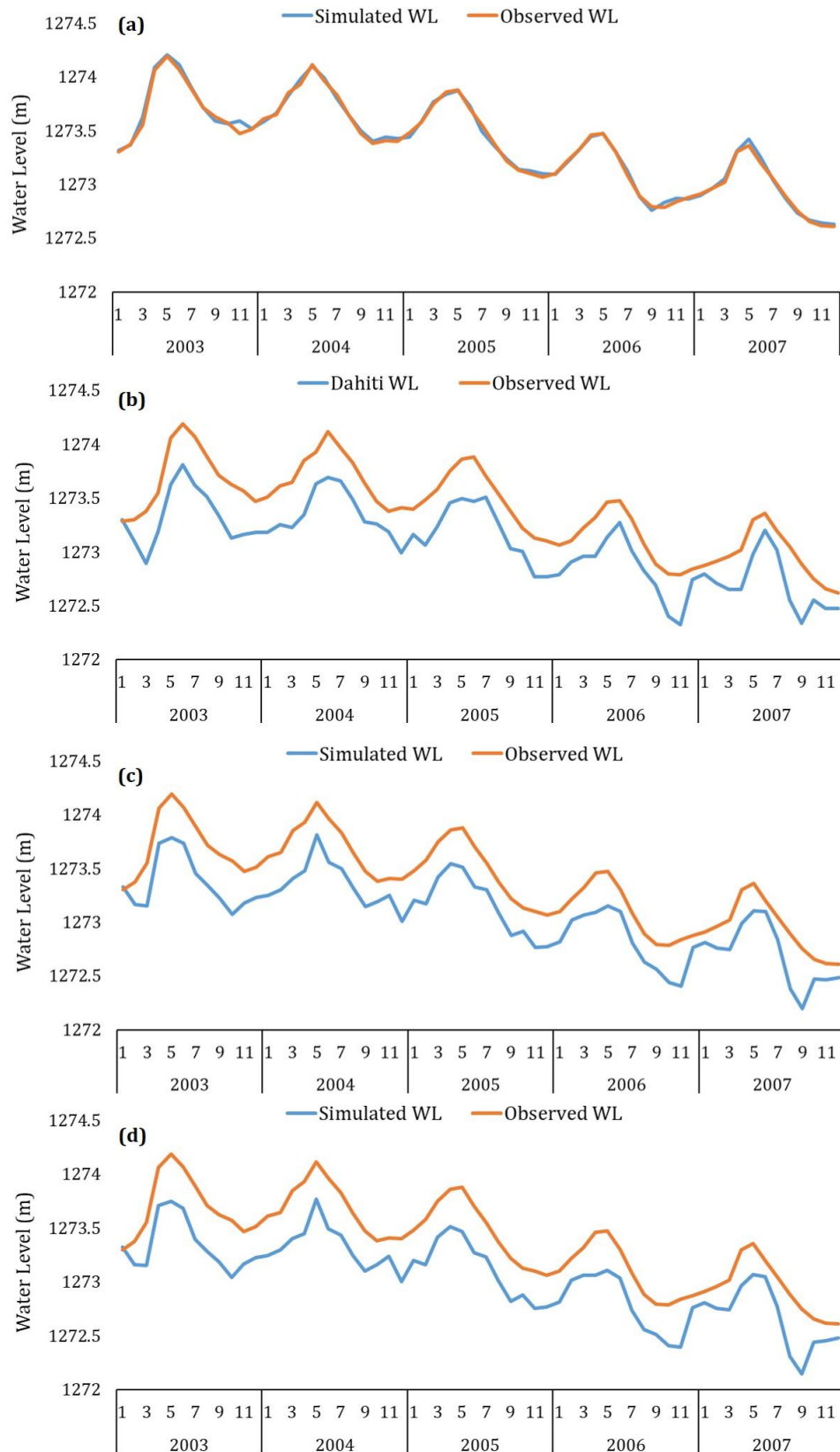
Figure 16. Monthly water level fluctuations. (a) Sc-01 based on combination of all observed data. (b) Sc-02 based on combination of DAHITI WL and observed WL. (c) Sc-03 based on combination of DAHITI WL and RS evaporation. (d) Sc-04 based on combination of all RS and observed rainfall data.

In June-July of each year (2003-2007), water level was considerably higher than all other months in all scenarios. Moreover, it is also visible that simulated WL based on Sc-01 show better pattern than other scenarios (Figure 16.a). For different scenarios, statistical assessment was also considered. The simulation WLF for four different scenarios showed considerable well correlation, particularly for scenario-1 (Figure 17 and Table 4).
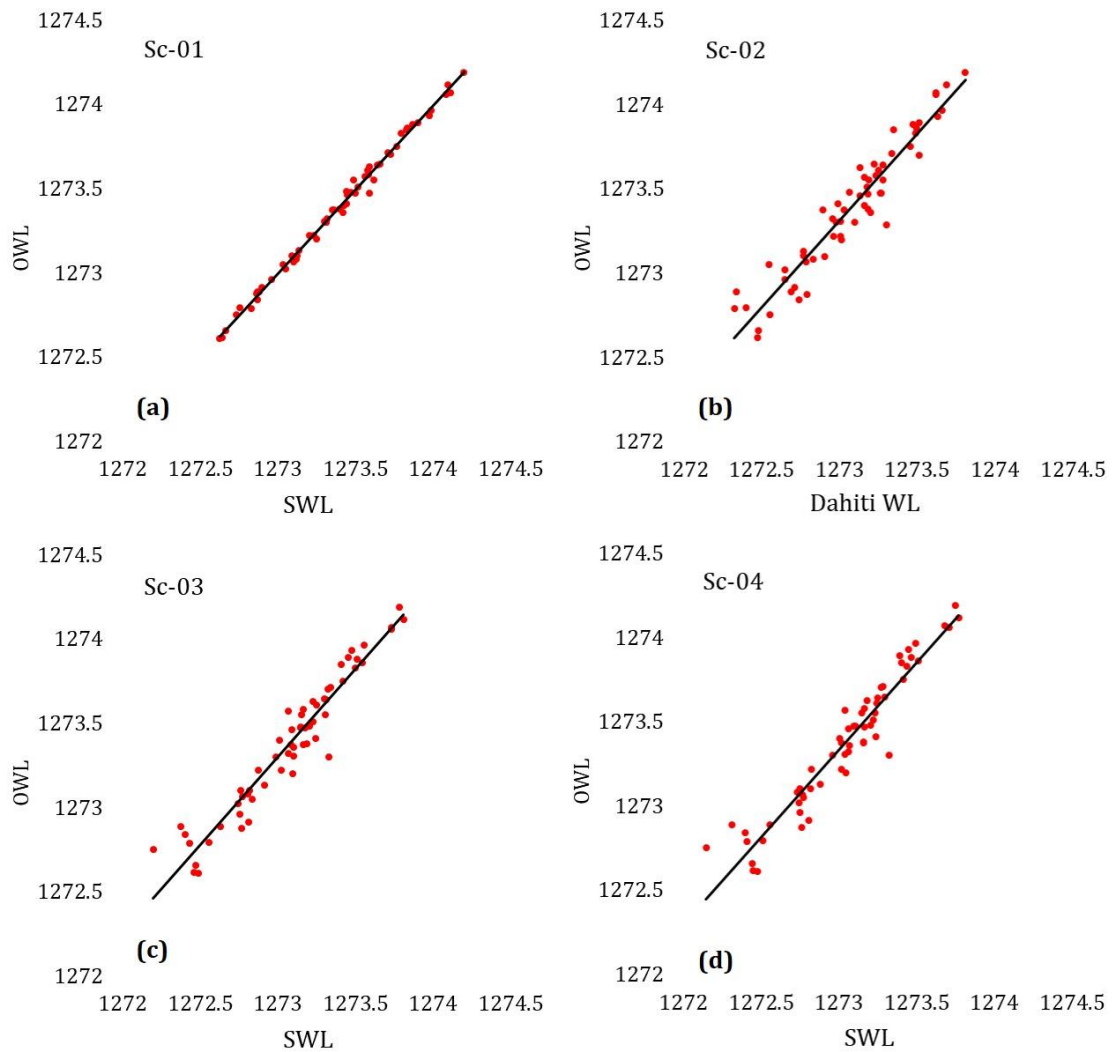

Figure 17. Correlation in between simulated and observed water level. (a) Sc-01. (b) Sc-02. (c) Sc-03. d) Sc-04.

The simulated WL in Sc-1 showed a well correlation with observed data ($R^2 = 0.99$, Figure 17.a and Table 4) whereas, simulated WL in other scenarios showed comparatively poor correlation (Figure 17 and Table 4).

Table 4. Statistical output results in for all scenarios.

Scenario	SSE	R-square	DF	Adjrsquare	rmse	m	b
SC-01	0.05	0.99	58.00	0.99	0.03	1.00	5.48
SC-02	0.78	0.91	58.00	0.91	0.12	1.03	-41.35
SC-03	0.71	0.93	58.00	0.93	0.11	1.04	-52.48
SC-04	0.81	0.92	58.00	0.92	0.12	1.04	-50.24

Moreover, it is also clear that the situation is fairly better in Sc-03, where it showed the effectiveness of remote sensing evaporation (Figure 17.c and Table 4). This proposition is also true for Sc-01 where it considers the input from all observed data.

4 DISCUSSION

The water level has been decreased in Lake Urmia in past few years based on available field stations (Figure 2). Remote sensing dataset of Lake Urmia also supports this proposition. (Torabi Haghighi & Kløve, 2015a), mentioned in their studies about the anthropogenic effects along with basin size, topography and lake size which are responsible for water level declination. Climatic variables like temperature, precipitation and evaporation also have considerable effect on water levels in Lake Urmia in last few decades.

Estimation of water level in lakes is quite challenging due to several factors (Schwatke et al., 2015a). For instance, for large lakes, the assumption of a lake area may no longer be addressable. Systematic errors in geophysical and ranges correction, wind and waves may also affect lake water level differences (Schwatke et al., 2015a). In this study, temporal changes of WLF were monitored by using Jason-2 and Jason-3 satellite altimetry missions. The estimated WLF did not show any specific pattern, because of data assimilation though in some cases it showed a better correlation. However, estimated WLF in case of Jason-2 (Figure 8 and Figure 10) showed higher WLF in first two sections of Lake Urmia and poor correlation rather than the third section of lake with respect to observed and DAHITI WL. The situation is not same in Jason-3. Estimated WLF in Jason-3 (Figure 11 and Figure 12) showed that second and third section of the lake had higher WLF and poor correlation with respect to DAHITI WL. The case is little bit better for first section of the lake.

The variations of water level in different parts of lake Urmia can be explained by (Torabi Haghighi et al., 2018a), where they considered no occurrence of outflow from the lake except evaporation. Lake Urmia also has higher annual evaporation than precipitation which make non uniformity of WLF (OWWMP, 2011). Another major issue is flow regime which varied to a certain extent in different climate patterns (Nilsson et al., 2005). Altimetry data also have systematic errors. Especially at large scales these errors can generate WLF for different sections within the lake (Schwatke et al., 2015a).

The results of evaporation in (Figure 13) showed observed evaporation have different variabilities throughout the year as they don't follow same trend. In 2003-2013, most of

the observed evaporation stations have well correlation with respect to remote sensing dataset (Figure 14). In case of monthly average ratio, Tabgolshi fresh evaporation station showed most consistency from January-December with RS evaporation in comparison to others (Figure 15 and Table 3). Based on the location and monthly ratio with respect to RS dataset, Tabgolshi fresh station was selected for scenario analysis; which is in North West corner of Lake Urmia.

Combination of multiple data sources showed good harmony with field water level of Lake Urmia. For Sc-1 simulated water level showed highest correlation ($R^2 = 0.99$, Figure 17.a) with observed WL. DAHITI WL also showed better similarity. Scenario analysis give an overview to understand the overall situation as well as response of Lake Urmia throughout the period. With the indication of this scenario analysis, it is also feasible from managerial point of view to take any future decision about water control and regulations in Lake Urmia.

5 CONCLUSION

Different satellite mission based water level estimation algorithm can explain the diversity of Lake water level fluctuations. For instance, Jason-2 and Jason-3 based water level estimation can lead us to explain altimetry for inland water bodies. Though in this study it is visible that in some cases the correlation between observed and satellite data was not in good harmony. However, the algorithm of estimating water level showed better pattern in case of some sections in Lake Urmia.

This study integrates multiple driving factors to analyse different scenarios by combining remote sensing and observed data with the application of water balance equation in Lake Urmia. Combination of different data sources explain the plausible causes of water level fluctuations. The analysis leads to a new insight to understand the temporal phenomenon of Lake Urmia. It also explains the necessity of using proper data sources to make decision about water regulations and managerial decisions.

6 REFERENCES

Abatzoglou, J.,Hegewisch, K. et al.(2016). Climate Engine.org.User Guide,53 (August).Retrieved from: https://webpages.uidaho.edu/jabatzoglou/TOOLS/DROUGHT/USERGUIDE/UserManual_ClimateEngine.pdf.

Abreham, A. (2009). Open Water Evaporation Estimation Using Ground Measurements and Satellite Remote Sensing : a case study of Lake Tana , Ethiopia. Thesis, (1-6), 106.

Adam Bolesław, L., & Anna, B. (2017). Current state of art of satellite altimetry. Retrieved from https://www.researchgate.net/publication/324915480_Current_State_of_Art_of_Satellite_Altimetry/link/5aeb24210f7e9b837d3c7d78/download.

Atanaw, F. (2009). Estimation of Water Balance Components Using Remote Sensing Products-in-the-Upper-Blue-Nile,Lake-Tana-Sub-Basin,(March),109. https://doi.org/10.3390/w10050657.

AVISO. (2017). Along-track Level-2 + (L2P) SLA Product Handbook, (September). Retrieved form https://www.aviso.altimetry.fr/fileadmin/documents/data/tools/hdbk_L2P_all_missions_except_S3.pdf.

Bracht-Flyr, B., Istanbulluoglu, E., & Fritz, S. (2013). A hydro-climatological lake classification model and its evaluation using global data. Journal of Hydrology, 486, 376–383. https://doi.org/10.1016/j.jhydrol.2013.02.003.

Brenner, A. C., Zwally, H. J., & Bentley, C. R. (2003). GLAS: Derivation of Range and Range Distributions From Laser Pulse Waveform Analysis for Surface Elevations, Roughness, Slope, and Vegetation Heights. Geoscience Laser Altimeter System (GLAS) Algorithm Theoretical Basis Document, vertion 4.(November 2011), 99. https://doi.org/10.1117/12.414116.

Bronner. E, Guillot. A, Picot.N, (2016). SARAL_Altika_products_handbook_v2.5_July 2016. CNES: SALP-MU-M-OP-15984-CN.Retrieved-from: https://www.aviso.altimetry.fr/fileadmin/documents/data/tools/SARAL_Altika_products_handbook_01.pdf.

Chelton, D. B. Ries, J. C., Haines, B. J., Fu, L. L., Callahan, P. S., 2001. Satellite altimetry International Geophysics . 69, 1-ii.

Chow-Fraser, P. (2005). Ecosystem response to changes in water level of Lake Ontario marshes: Lessons from the restoration of Cootes Paradise Marsh. Hydrobiologia, 539(1), 189–204. https://doi.org/10.1007/s10750-004-4868-1.

Crapper, P. F., Fleming, P. M., & Kalma, J. D. (1996). Prediction of lake levels using water-balance-models.Environmental-Software,11(4),251–258. https://doi.org/10.1016/S0266-9838(96)00018-4.

Desai, S. D. (2002). Observing the pole tide with satellite altimetry. Journal of Geophysical Research, 107 (C11), 3186. http: doi.org/10.1029/2001JC001224.

Dingman S.L. (2002). Physical hydrology. Prentice Hall, Upper Saddle River, 646 pp.

Dubey, A.K., Gupta, P.K., Dutta, S., & Singh, R.P.(2015). An improved methodology to estimate river stage and discharge using Jason-2 satellite data. Journal of Hydrology, 529, 1776-1787. https://doi.org/10.1016/j.jhydrol.2015.08.009.

Dumont, J, Rosmorduc, V, Picot, N, Desai, S et al. (2009a). OSTM/Jason-2. Products Handbook. CNES: SALP-MU-M-OP-15815-CN, EUMETSAT: EUM/OPS-JAS/MAN/08/0041, JPL: OSTM-29-1237, NOAA/NESDIS: Polar Series/OSTM, 400:1.

Dumont, V. Rosmorduc, L. Carrere, N. Picot, H. Bonekamp, S. et al. (2016b). OSTM/Jason-3 Products Handbook. CNES: SALP-MU-M-OP-16118-CN. EUMETSAT: TBD, JPL: TBD, NOAA/NESDIS: TBD.

Esa. (2007). ENVISAT RA2/MWR Product Handbook. Report: Retrieved from https://earth.esa.int/pub/ESA_DOC/ENVISAT/RA2-MWR/ra2-mwr.ProductHandbook.2_2.pdf.

Eimanifar, A., & Mohebbi, F. (2007). Urmia Lake (northwest Iran): A brief review. Saline Systems, 3(1), 5.

Esa.earth online. Terra/Aqua MODIS(2000). Explore earth online Web site. Retrived from https://earth.esa.int/web/guest/missions/3rd-party-missions/current-missions/terraaqua- modis.

Ecenur, C. (2016). Multi-temporal water extent analysis of a hypersaline playa lake using landsat imagery. IOSR Journal of Economics and Finance, 3(1), 56. https://doi.org/https://doi.org/10.3929/ethz-b-000238666.

Fazel, N., Torabi Haghighi, A., & Kløve, B. (2017). Analysis of land use and climate change impacts by comparing river flow records for headwaters and lowland reaches. Global and Planetary Change, 158(September), 47–56. https://doi.org/10.1016/j.gloplacha.2017.09.014.

Ferguson, H. A. (1981). Methods of Computation of Water Balance of Large Lakes and Reservoirs, Volume I Methodology, A Contribution to IHP, Studies and Reports in Hydrology 31, UNESCO Publications, Paris.

Global Runoff Data Centre (GRDC): Long- Term Mean Monthly Discharges and Annual Characteristics of GRDC Station/Global Runoff Data Center, Federal Institute of Hydrology (BfG), Koblenz, Germany, 2013.

Hofmann, H., Lorke, A., & Peeters, F. (2008). Temporal scales of water-level fluctuationsin lakes and their ecological implications. Hydrobiologia 613, 85–96.https://doi.org/10.1007/s10750-008-9474-1

Hopfield, H. (1971). Tropospheric effect on electromagnetically measured range: Prediction from surface weather data. Radio Science, 6(3):357–367. doi:10.1029/RS006i003p00357.

Laurens, M., Bouwer, T. W. B. & JeroenC. J. H. A. (2008). Estimates of spatial variation in evaporation using satellite-derived surface temperature and a water balance model. Human Nature, 1245 (March), 1243-1245 https://doi.org/10.1002/hyp.

Lemoine, F. G., Kenyon, S. C., Factor, J. K., Trimmer, R. G., Pavlis, N. K., Chinn, D. S.,others. (1998). The development of the joint NASA GSFC and the NIMA geopotential model EGM96, NASA Goddard Space Filght Center. Greenbelt, Maryland, 20771(July).

Mercier, F., Rosmorduc, V., Carrere, L., & Thibaut, P. (2010). Coastal and Hydrology Altimetry product (PISTACH) handbook, 64.

Modares, F. (2018). The role of climate and land use change in Lake Urmia desiccation. Retrieved-from http://jultika.oulu.fi/files/isbn9789526221021.pdf.

Mehta, V. M., Decandis, A. J., & Mehta, A. V. (2005). Remote-sensing-based estimates of the fundamental global water cycle: Annual cycle. Journal of Geophysical Research Atmospheres, 110(22), 1–14. https://doi.org/10.1029/2004JD005672.

Mcshane, R. R., Driscoll, K. P., & Sando, R. (2017). A Review of Surface Energy Balance Models for Estimating Actual Evapotranspiration with Remote Sensing at High Spatiotemporal Resolution over Large Extents - Scientific Investigations Report-2017–5087.Scientific-Investigations-Report,19. https://doi.org/https://doi.org/10.3133/sir20175087.

Melesse, A. M., Abtew, W., & Dessalegne, T. (2009). Evaporation estimation of Rift Valley lakes: Comparison of models. Sensors, 9(12), 9603–9615. https://doi.org/10.3390/s91209603.

Morrill, C., Small, E. E., & Sloan, L. C. (2001). Modeling orbital forcing of lake level change: Lake Gosiute (Eocene), North America. Global and Planetary Change, 29(1–2), 57–76. https://doi.org/10.1016/S0921-8181(00)00084-9.

Nilsson, C., Reidy, C. A., Dynesius, M., & Revenga, C. (2005). Fragmentation and flow regulation of the world's large river systems. Science, 308(5720), 405–408. https://doi.org/10.1126/science.1107887.

Nouri, H., Mason, R. J., & Moradi, N. (2017). Land suitability evaluation for changing spatial organization in Urmia County towards conservation of Urmia Lake. Applied Geography, 81, 1–12. https://doi.org/10.1016/j.apgeog.2017.02.006.

Okeowo, M. A., Lee, H., Hossain, F., & Getirana, A. (2017). Automated Generation of Lakes and Reservoirs Water Elevation Changes from Satellite Radar Altimetry. IEEE Journal of Selected Topics in Applied Earth Observations and Remote Sensing, 10(8), 3465–3481. https://doi.org/10.1109/JSTARS.2017.2684081.

OWWMP. (2011). Iran Ministry of Energy's Office for Water and Wastewater Macro Planning. Iran's comprehensive water resources plan. Meteorological Report,, 2385070–44.

Richter, B. D., & Thomas, G. A. (2007). Restoring environmental flows by modifying dam operations. Ecology and Society, 12(1).https://doi.org/10.5751/ES-02014-120112.

Rokni, K., Ahmad, A., Selamat, A., & Hazini, S. (2014). Water feature extraction and change detection using multitemporal landsat imagery. Remote Sensing, 6(5), 4173–4189. https://doi.org/10.3390/rs6054173.

Roman, D. R., Wang, Y. M., Saleh, J., & Li, X. (2010). Geodesy, geoids, and vertical datums: A perspective from the US National Geodetic Survey. FIG Congress, (April),11–16.Retrievedfrom http://fig.net/pub/fig2010/papers/ts01c%5Cts01c_roman_wang_et_al_3768.pdf.

Rosenberg, D. M., Mccully, P., & Pringle, C. M. (2000). Global-Scale Environmental Effects of Hydrological Alterations: Introduction. BioScience, 50(9), 746. https://doi.org/10.1641/0006-3568(2000)050[0746:gseeoh]2.0.co;2.

Schwatke, C., Dettmering, D., Bosch, W., & Seitz, F. (2015a). DAHITI - An innovative approach for estimating water level time series over inland waters using multi-mission satellite altimetry. Hydrology and Earth System Sciences, 19(10), 4345–4364. https://doi.org/10.5194/hess-19-4345-2015.

Schwatke, C., Dettmering, D., Bosch, W., and Seitz, F. (2016b). Database for Hydrological, (November).

Senay, G. B., Budde, M., Verdin, J. P., & Melesse, A. M. (2007a). A coupled remote sensing and simplified surface energy balance approach to estimate actual evapotranspiration from irrigated fields. sensors, 7(6), 979–1000. https://doi.org/10.3390/s7060979.

Senay, G. B., Leake, S., Nagler, P. L., Artan, G., Dickinson, J., Cordova, J. T., & Glenn, E. P. (2011b). Estimating basin scale evapotranspiration (ET) by water balance and remote-sensing-methods.Hydrological-Processes,-25(26),4037–4049. https://doi.org/10.1002/hyp.8379.

Su, Z. (2002). The Surface Energy Balance System (SEBS) for estimation of. Hydrology and Earth System Sciences,, 6(1), 85–99.

Senay, G. B., Bohms, S., Singh, R. K., Gowda, P. H., Velpuri, N. M., Alemu, H., & Verdin, J. P. (2013c). Operational Evapotranspiration Mapping Using Remote Sensing and Weather Datasets: A New Parameterization for the SSEB Approach. Journal of the American Water Resources Association, 49(3), 577–591. https://doi.org/10.1111/jawr.12057.

Sima, S., & Tajrishy, M. (2013). Using satellite data to extract volume-area-elevation relationships for Urmia Lake, Iran. Journal of Great Lakes Research, 39(1), 90–99. https://doi.org/10.1016/j.jglr.2012.12.013.

Soja, G., Züger, J., Knoflacher, M., Kinner, P., & Soja, A. M. (2013). Climate impacts on water balance of a shallow steppe lake in Eastern Austria (Lake Neusiedl). Journal of Hydrology, 480, 115-124. https://doi.org/10.1016/j.jhydrol.2012.12.013.

Sui, X., Zhang, R., Wu, F., Li, Y., & Wan, X. (2017). Sea surface height measuring using In SAR altimeter. Geodesy and Geodynamics, 8 (4), 278-284. https://doi.org/10.1016/j.geog.2017.03.005.

Torabi Haghighi, A., Fazel, N., Hekmatzadeh, A. A., & Klöve, B. (2018a). Analysis of Effective Environmental Flow Release Strategies for Lake Urmia Restoration. Water Resources Mangement, 32 (11), 3595-3609. https://doi.org/10.1007/s11269-018-2008-3.

Torabi Haghighi, A., Menberu, M. W., Aminnezhad, M., Marttila, H., & Kløve, B. (2016b). Can lake sensitivity to desiccation be predicted from lake geometry? Journal of Hydrology, 539, 599-610 https://doi.org/10.1016/j.jhydrol.2016.05.064.

Torabi Haghighi, A., & Kløve, B. (2015a). A sensitivity analysis of lake water level response to changes in climate and river regimes. Limnologica, 51, 118–130. https://doi.org/10.1016/j.limno.2015.02.001.

Torabi Haghighi, A., & Kløve, B. (2017b). Design of environmental flow regimes to maintain lakes and wetlands in regions with high seasonal irrigation demand. Ecological-Engineering,-100,120–129. https://doi.org/10.1016/j.ecoleng.2016.12.015.

Tourian, M. J., Sneeuw, N., & Bárdossy, A. (2013a). A quantile function approach to discharge estimation from satellite altimetry (ENVISAT). Water Resources Research, 49(1-13), 4174–4186. https://doi.org/10.1002/wrcr.20348.

Tourian, M. J., Elmi, O., Chen, Q., Devaraju, B., Roohi, S., & Sneeuw, N. (2015b). A spaceborne multisensor approach to monitor the desiccation of Lake Urmia in Iran. Remote-Sensing-of-Environment,-156,-349–360. https://doi.org/10.1016/j.rse.2014.10.006.

Tsubo, M., Fukai, S., Tuong, T. P., & Ouk, M. (2007). A water balance model for rainfed lowland rice fields emphasising lateral water movement within a toposequence. Ecological Modelling, 204 (3-4), 503-515 https://doi.org/10.1016/j.ecolmodel.2007.02.001.

Velpuri, A., G.B. Senay, B., R.K. Singh, A., S. Bohms, C., J. P. V. pd. (2013). A comprehensive evaluation of two MODIS evapotranspiration products over the conterminous United States: Using point and gridded FLUXNET and water balance ET.

World Commission on Dams (WCD), (2000). Dams and development: A new framework for decision-making. Earthscan Publications, London, UK.

Wahr, J. M. (1985). Deformation induced by polar motion. Journal of Geophysical Research, 90 (B11), 9363-9368. https://doi.org/10.1029/JB090iB11p09363.

Xu, H. (2006). Modification of normalized differences water Index (NDWI) to enhance open water features in remotely sensed imagery, 17 (14), 3025-3033.